

Exploring Natural Product Biosynthesis in *Photorhabdus laumondii*: A Novel Strategy through Activation of Bacterial Enhancer Binding Proteins

Lydia Rili

A Thesis
in the Department of
Chemistry and Biochemistry

Presented in Partial Fulfillment of the Requirements
for the Degree of
Master of Science (Biochemistry)

at Concordia University
Montréal, Québec, Canada

April 2024
© Lydia Rili, 2024

CONCORDIA UNIVERSITY
School of Graduate Studies

This is to certify that the thesis prepared

By: Lydia Rili
Entitled: **Exploring Natural Product Biosynthesis in Photorhabdus laumondii:
A Novel Strategy through Activation of Bacterial Enhancer Binding Proteins**

and submitted in partial fulfillment of the requirements for the degree of

Master of Science (Biochemistry)

complies with the regulations of the University and meets the accepted standards with respect to originality and quality.

Signed by the final examining committee:

_____ Chair
Dr. Peter Pawelek

_____ Examiner
Dr. Malcolm Whiteway

_____ Examiner
Dr. Peter Pawelek

_____ Thesis Supervisor(s)
R. Brandon Findlay

_____ Thesis Supervisor(s)

Approved by _____
Dr. Louis Cuccia Graduate Program Director

Dr. Pascale Sicotte Dean of Arts & Science

Abstract

Exploring Natural Product Biosynthesis in *Photorhabdus laumondii*: A Novel Strategy through Activation of Bacterial Enhancer Binding Proteins

Lydia Rili

It has been reported that the number of known natural products is much less than the number of biosynthetic gene clusters (BGCs) found in the genomes of microorganisms, which suggests a considerable potential for new drug discovery. However, a significant challenge arises as these BGCs cannot be induced in a laboratory setting. Due to high fitness cost for bacteria, these encoded natural products are tightly regulated. Consequently, our limited understanding of the triggers and regulatory mechanisms of these BGCs impedes progress in the search for potential antibiotics.

To tackle this issue, we propose an alternative approach distinct from the traditional methods such as high-throughput screening, heterologous expression, or the introduction of constitutive promoters. Our strategy involves using the bacterial machinery to activate the expression of BGCs by constitutively activating their bacterial enhancer binding proteins (bEBPs). This is achieved by deleting the regulatory domain located at the N-terminal of bEBPs. The majority of these bEBPs are responsible for activating the σ^{54} -RNA polymerase holoenzyme, thereby initiating transcription.

We have demonstrated σ^{54} 's importance in regulating the expression of a wide range of natural products in *Photorhabdus laumondii*. This was achieved by utilizing the core domain of DctD (DctD₍₁₄₁₋₃₉₄₎), a bEBP from *Sinorhizobium meliloti*. Further examination of the modified *P. laumondi* bEBP (mEBPs) revealed diverse effects on natural product expression involving activation and/or repression. Some of these mEBPs exhibit elevated expression levels and, in certain instances, demonstrate propensity for specific natural products compared to DctD₍₁₄₁₋₃₉₄₎. These preliminary findings suggest that mEBPs, could in time enable us to selectively express a subset of σ^{54} -dependent BGCs. This would bypass the need for specific growth conditions, unlocking a reservoir of previously inaccessible natural products.

Acknowledgements

I wish to express my heartfelt thanks to all those who have contributed throughout my Master's journey. It has been marked by challenges, successes, late nights, and moments of joy, all of which have shaped me into the person I am today.

First, I extend my appreciation to Dr. Brandon Findlay for his consistent support and invaluable guidance. His mentorship has provided me with insights into what it is to be a scientist.

I am grateful to my colleagues and lab members, past and present, for their friendship, strength, and shared laughter during both the highs and lows of our research journeys. Special thanks are due to Laura Dominguez, Nathalie Read, Perna Singh, Farhan Rahman Chowdhury, Michael Mahdavi, and Sylvie Ouellette for their unwavering emotional support and invaluable assistance throughout my journey.

Furthermore, I am grateful to Dr. Helge Bode for graciously sharing his conjugation protocol, Heng Jiang for his expertise in LC-MS analysis, and Sylvie Ouellette and Farhan Rahman Chowdhury for their proofreading efforts. My gratitude also extended to Perna Singh for plasmid sequencing, Gabriel Aguiar-Tawil for obtaining strains, and the Fernandez Herrero Lab at the National Centre for Biotechnology in Madrid for generously providing strains.

I am thankful to my committee members, Dr. Malcolm Whiteway and Dr. Peter Pawelek, for their invaluable feedback and guidance throughout my MSc. Additionally, I am grateful to Dr. Louis Cuccia for his encouragement, and to Concordia University for fostering an environment conducive to academic growth and learning.

Finally, I am deeply thankful to my family for their unwavering support and encouragement. Special thanks to my parents, Rabah Rili and Zahia Abderrahim, for their belief in my potential, and to my brother, Anis Rili, for his constant support and assistance with proofreading.

This journey would not have been possible without the support, guidance, and encouragement of all those mentioned above. Thank you for being an integral part of my academic and personal growth.

Contributions of Authors

Lydia Rili: Wrote the first draft of this thesis and corrected subsequent versions. Performed all listed experiments and analyses.

Brandon Findlay: Project supervisor responsible for correcting the manuscript. Performed an antiSMASH analysis that identified the bacterial strain used in this study.

Copyright information

The data presented in this thesis will be adapted for a publication in a near future.

Table of Contents

LIST OF FIGURES	VII
LIST OF TABLES	VIII
LIST OF ABBREVIATION	IX
INTRODUCTION	1
Natural products	1
NPs, Advantages and Drawbacks.....	1
NPs and their Biosynthetic Gene Clusters	2
NPs potential: Exploring Conventional Methods.....	3
NPs Explored: Delving into the potential of <i>Photorhabdus</i> spp.....	4
NPs production: Unraveling the Role of σ^{54} in Transcription.....	5
NPs Regulation: Understanding the Function of bEBPs.....	6
Investigating NP expression via a novel approach employing bEBPs.....	8
MATERIALS AND METHODS	9
Bioinformatics	9
Strains and Plasmids.....	9
Media and Chemicals	10
EBPs modification (mEBPs) and recombinant plasmid construction.....	11
mEBP variants generation.....	13
NP production, extraction, and analysis protocols.....	14
Knockout Cassettes	16
RESULTS	17
Bioinformatic analysis.....	17
1. Strain selection	17
2. bEBPs identified in <i>P. laumondii</i> TTO1	18
Generating variants.....	19
Effect of mEBPs on Cell Growth	20
Assessing the effect of DctD ₍₁₄₁₋₃₉₄₎ on NP biosynthesis.....	21
1. Effect on metabolite expression	21
2. Effect on NP expression	22
Assessing the effect of mEBPs on NP biosynthesis.....	28
1. Effect on metabolite expression	28
2. Effect on NP expression	30
DISCUSSION	33
REFERENCES:	41
APPENDIX	49
List of supporting Figures and Tables.....	49

List of Figures

Figure 1. bEBP mechanism of action. ³¹	7
Figure 2. pARO190 map.	10
Figure 3. BGCs' distribution amongst <i>Gammaproteobacterial</i> families.	17
Figure 4. cPCR confirmation of pARO190-tyrR _(Δ2-123) conjugation.....	20
Figure. 5. Effect of DctD ₍₁₄₁₋₃₉₄₎ on metabolites expression in <i>P. laumondii</i> TTO1.	22
Figure 6. PL-A identification.....	23
Figure 7. AQ-270 identification.	24
Figure 8. PPY-D identification.	25
Figure 9. GXP-A identification.....	25
Figure 10. IPS identification.....	26
Figure 11. MVAP-A identification.....	27
Figure 12. Effect of DctD ₍₁₄₁₋₃₉₄₎ on NPs expression levels in <i>P. laumondii</i> TTO1.	28
Figure 13. Effects of mEBPs on metabolite expression in <i>P. laumondii</i> TTO1.....	29
Figure 14. Effect of mEBPs on NPs expression levels in <i>P. laumondii</i> TTO1.....	32

List of Tables

Table 1. Bacterial strains and plasmids used in this study.	10
Table 2. Modified bEBPs used in this work.	12
Table 3. Primers used to generate mEBPs.	13
Table 4. PCR settings used in this study.	13
Table 5. Primers used to confirm strains or plasmid identity.	14
Table 6. PCR cycle used in this study.	16
Table 7. Identified σ_{54} -dependent bEBPs in <i>P. laumondii</i> TTO1.	18
Table 8. Variants phenotypic categorization.	21
Table 9. Compounds to be analysed in this study.	22
Table 10. Summary of findings for each constrictively active EBP.	36

List of abbreviation

- NP Natural Product
- BGC Biosynthetic Gene Cluster
- bEBP bacterial Enhancer Binding Protein
- dsDNA double-stranded DNA
- DctD C₄-dicarboxylic acid transport protein D
- mEBP modified EBP
- R domain Regulatory domain
- C domain Core (AAA+) domain
- D domain DNA binding domain
- LB/LA Lysogeny Broth/Agar
- TSB/TSA Tryptic Soy Broth/Agar
- PCR Polymerase Chain Reaction
- cPCR colony PCR
- ON Overnight
- WT Wild Type
- LC-MS Liquide Chromatography Mass Spectrometry
- MVAP-A Mevalagmapeptide A
- PL-A Phurealipid A
- PPY-D Photopyrone D
- IPS Isopropylstilbene
- AQ 270 Anthraquinone 270
- GXP-A GameXpeptide A
- RT Retention Time
- PH Peak Hight
- Y Yellow
- B Beige

INTRODUCTION

Natural products

Natural products (NPs) which include secondary metabolites, are small molecules or proteins that are considered non-essential for growth but crucial for development under stressful conditions^{1,2}. In response to various environmental challenges, microorganisms have adapted to produce a diverse range of NPs. These challenges include the need for communication, both intra- or interspecies to regulate a colony-wide response to the surrounding stimuli³. An illustration of that is evident in the symbiotic interaction of bacteria with its host, which may lead to fostering host growth^{4,5}. Nonetheless, our interest in these NPs lies in their bioactive properties, such as their ability to inhibit, deter or kill similar or closely related microbes perceived as competitors or prey^{1,2,4,6,7}.

NPs, Advantages and Drawbacks

In pharmacology these bioactive NPs are very important. They are used in modern medicine as antibiotics, biocontrol agents against food spoilage by fungi, as well as therapeutic treatments like anti-cancer drugs and immunosuppressants^{2,4,8-10}.

Our primary objective behind the development of different antibiotics is to combat bacterial infections¹¹. However, as our usage of antibiotics increases, so does the surge in multidrug bacterial resistance^{8,12}. We can observe this resistance through the different bacterial strategies implemented in response to this new hostile environment. These strategies include horizontal acquisition of resistance genes and local modification of foreign molecules^{5,11}. However, the most common mechanism of resistance is up-regulation of specific genes encoding

for transporters or permeases as well as efflux pumps to remove antibiotics that permeated the bacterial cell wall^{5,11,13}. Combined, these approaches limit the transport of antibiotics into the cell, providing broad-spectrum resistance at minimal cost.

It is predicted that by 2050 the leading cause of death would be through bacterial infections which would be permitted to proliferate due to antibiotic resistance¹². The life losses would be numbered in the tens of millions, with a considerable impact on our health care system and livelihood¹². Hence, the renewed global interest in further exploring the bacterial genome and identifying new NPs with antibacterial activity^{8,9}.

NPs and their Biosynthetic Gene Clusters

In most complex eukaryotes, each gene falls under the control of complex levels of regulation to obtain one final protein product¹⁴. Prokaryotes, on the other hand express their genes as a group under the control of one set of regulatory elements to yield multiple proteins¹⁴. These secondary metabolite-encoding genes are physically clustered by function in packages referred to as biosynthetic gene clusters (BGCs). These functions include regulation, co-factor biosynthesis, transport elements and self-resistance, all expressed for the production and the proper function of multiple bioactive NPs and/or proteins at once.¹⁴⁻¹⁶

Some of these BGCs are believed to be cryptic. Their cognate NPs have yet to be identified since they are difficult to be expressed in standard laboratory growth conditions⁸. This issue is caused by either heavy regulation, expression below our detection limit, or more importantly we have yet to uncover all the cues and triggers required for their activation.^{1,8,9,17,18}

NPs potential: Exploring Conventional Methods

Many traditional technologies focus on different aspect of this issue. To mine for new NPs, some allow for a successful reading of the BGCs and others for the identification of some components through large screening¹⁹. Amongst these technologies are:

High-throughput screening. In this approach, libraries of millions of compounds are tested with the aim of identifying elicitors that would successfully induce silent promoters^{19,20}. According to Mao et al. this approach is typically carried out by introducing a reporter gene downstream of a silent native promoter and exposing the modified strain to multiple elicitors independently. The goal as stated before is to identify one or more molecules that can be used as an inducer on the native strain to trigger the targeted BGC.²⁰

Heterologous expression. This strategy consists of constructing a vector carrying a cryptic BGC (otherwise silent in its native strain) and transforming it into a heterologous host, which was genetically modified usually through genome minimization or metabolite simplification (usually *Escherichia coli*) to elicit its expression. Upon obtaining the cognate NP(s), bioassay testing is conducted to determine the toxicity of the compound(s).^{4,21–23}

Promotor swapping. This approach involves the introduction of a constitutive promoter upstream of the cryptic BGC and controllably inducing its expression. This technique requires that the genome of the explored strain be already annotated and sequenced.²⁰

These strategies have helped to unlock the NP potential of many strains. However, they are time-consuming, and most of them overlook key molecules found in the native strains. These molecules could be substrates or co-factors that are required for the proper activation of these cryptic BGCs and functioning of their proteins.^{1,17,20,24}

NPs Explored: Delving into the potential of *Photorhabdus* spp.

Prior to this study different *Gammaproteobacterial* families were examined. The *Photorhabdus* genus, an *Enterobacterales* order of Gram-negative bacteria, specifically *P. laumondii* subsp. *laumondii* TTO1, was selected due to its availability and the presence of 22 BGCs (our unpublished data). We will be exploring *P. laumondii* TTO1, a model entomopathogenic bacteria with a genome size of 5.69 megabase pairs (Mbp), which carries up to 4,839 protein-coding genes, some of which have yet to be characterized^{1,24,25}.

Photorhabdus is an entomopathogenic bacteria which has a fascinating and complex lifecycle^{26,27}. A well-studied aspect of its lifecycle is its relationship with its hosts which can be separated in two forms. It is reported that these forms display distinct NP profiles and phenotypes, which could be referred to as phenotypic heterogeneity²⁷. During its pathogenic form (P-Form), *Photorhabdus* is in the active phase which correlates with its exponential growth phase and consists of two types of host-relationships⁵. The first is a mutualistic symbiont relationship with *Heterorhabditis bacteriophora*^{5,27}, a species of soil dwelling nematode. In contrast, the second relationship is infectious. *Photorhabdus* is released by the nematodes inside its prey, commonly the wax moth *Galleria mellonella* insect larvae, to kill and sterilize. This provides the bacteria and the nematodes with a food source to support their growth and reproduction^{5,27,28}. As the nematode reproductive cycle starts, a genetic locus in *Photorhabdus* called *madswitch* (maternal adherence switch) is activated. With the *madswitch* ON, a change of form (M-Form) occurs where the bacteria stick to and invade the gut of the mother nematode. This ensures its presence in the developing generation of infective juveniles (IJ).²⁷

The two forms are distinct. When the *madswitch* is OFF, *Photorhabdus* is in its P-Form which is necessary for the development and growth of the nematode as well as insect larvae

infection^{27,28}. It forms large pigmented colonies which express an array of NPs, including antibiotics and crystal inclusion bodies^{5,26}. In contrast, when the *madswitch* is ON, the bacteria switches to the M-Form; a less active phase required for its transmission to the developing IJ²⁷. This form is reported to consist of small unpigmented colonies with no antibiotic production and no infection or growth support function.²⁷

In our investigation of this fascinating bacteria, we have confirmed the presence in its genome of all the elements required for NP expression using transcriptional activators also known as bacterial enhancer binding proteins (bEBPs). Their presence is essential for the continuation of this study.

NPs production: Unraveling the Role of σ^{54} in Transcription

In bacteria, transcription is initiated by the activation of the sigma factors-RNA polymerase (σ -RNAP) holoenzyme complex^{16,29-31}. Different sigma factors are found to regulate the transcription of different groups of BGCs, and can be separated in two classes^{30,31}. First, the σ^{70} family holds housekeeping sigma factor and is responsible for the majority of transcription initiated during growth^{31,32}. The second class is represented by sigma factors structurally related to σ^{70} , known as σ^{54} , which regulate diverse responses to environmental stimuli³¹⁻³³. Both classes direct the holoenzyme complex to bind to a promoter region located at the start of the gene^{30,31}. Each of the two classes have a conserved promoter element binding sequence³¹. Some members of the σ^{70} family, when associating with RNAP, bind to a specific consensus sequence at positions -35 (TTGACA) and -10 (TATAAT); whereas σ^{54} has its own conserved and function critical consensus sequence at positions -24 (GG) and -12 (TGC)³¹.

After binding to the promoter elements, the σ^{70} holoenzyme is able to initiate transcription

readily through the isomerization of the double-stranded DNA (dsDNA)³¹. However, the σ^{54} holoenzyme must enlist the assistance of a bEBP, to help it convert its initial energetically favorable closed complex to an open one³¹. It is this latter key feature that we explore in this study: the important role that these σ^{54} -dependent bEBPs have in controlling the expression of different NPs.

σ^{54} has a distinct structure that is composed of three regions. Region I, found at the N-terminus, is responsible for binding to the bEBPs. Region II doesn't seem to play an essential role, its function has yet to be determined³¹. Finally region III located at the C-terminus, is a conserved region and is responsible for binding to the promoter element at position -24 as well as binding to the RNAP core^{30,31}. As the holoenzyme forms, σ^{54} directs it to bind loosely and in a closed conformation to the conserved promoter elements at the start of the σ^{54} -dependent genes^{30,31,34}. The -12 element is essential since this is the specific region where the melting of the dsDNA takes place to initiate transcription.³¹ In the inactive form of the holoenzyme (the closed conformation), σ^{54} binds to the -12 elements and blocks the dsDNA from melting. It is only by interacting with a bEBP at a conserved GAFTGA motif that this inhibitory binding can be released. This interaction causes a conformational change that switches the holoenzyme into an open complex which initiate the dsDNA melting process and thus transcription.³¹

NPs Regulation: Understanding the Function of bEBPs

As discussed, bEBPs are proteins that are required to convert the closed σ^{54} -RNAP holoenzyme complex into an open one^{30,31}. Many bEBPs are composed of 3 domains; a regulatory (R) domain, a AAA+ central (C) domain and a DNA binding (D) domain. Transcriptional activation usually requires the detection by the R domain of environmental cues through a signal

transduction cascade³¹. This leads to phosphorylation of the R domain, ligand binding and/or protein-protein interaction, all of which will in turn induce a conformational change in the C domain that will activate the bEBP³¹. This latter change in the C domain will generally promote as seen in Figure 1A, bEBP hexamer self-assembly and binding through its oligomerized D domains to the upstream activator sequence (UAS or enhancer site). The interaction of σ^{54} -RNAP holoenzyme to the active bEBP oligomer is facilitated by DNA looping (Figure 1B). Upon ATP hydrolysis, the bEBP- σ^{54} (-RNAP) interaction tightens, leading to a conformational change in the σ^{54} -RNAP and the melting of the dsDNA, thus initiating transcription (Figure 1C). This general sequence of activation can be observed with C₄-dicarboxylic acid transport protein D (DctD), a well-studied bEBP.³¹

bEBPs in their inactive form are normally dimeric. Usually, a functional bEBP oligomer (hexamer) is composed of 3 dimers. As indicated previously each monomer is composed of three domains³¹. Of these, only the C domain is required for activity.³⁵

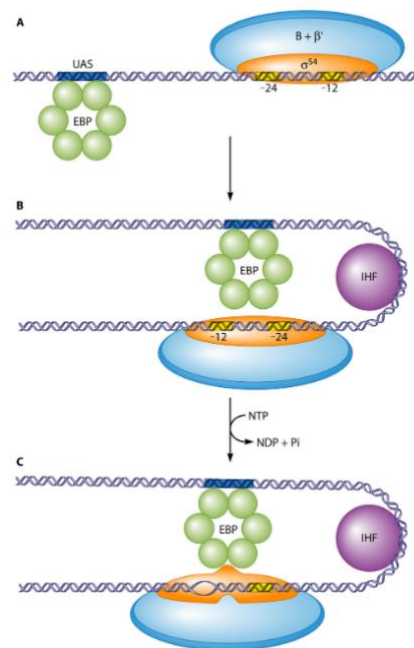


Figure 1. bEBP mechanism of action.³¹

Investigating NP expression via a novel approach employing bEBPs

Through this study, we will demonstrate that when rendered constitutively activated bEBPs endogenous to *P. laumondii* TTO1 activate NP biosynthesis. This approach bypasses the need for cues and heterologous expression, in principle greatly accelerating the discovery of new NPs. Furthermore, we will confirm, through the expression of DctD C domain (DctD₍₁₄₁₋₃₉₄₎), that σ^{54} is an important global regulator in *P. laumondii* TTO1 responsible for the expression of numerous BGCs.

MATERIALS and METHODS

Bioinformatics

An AntiSMASH³⁶ analysis was performed by Dr. Brandon Findlay , under default settings, comparing to the database the genome of different Gram-negative bacterial species to identify new BGCs. These genomes were uploaded from the publicly available database, NCBI. A type strain with a high count of new BGCs was identified and used for this study.

An NCBI pBLAST analysis was performed to identify bEBPs present in the selected strain's genome. The protein sequence of *Sinorhizobium meliloti* DctD core domain (DctD₍₁₄₁₋₃₉₄₎) was used as a template. The bEBPs identified were used in subsequent experiments.

Strains and Plasmids

All the strains and plasmids used are listed in Table 1. *Escherichia coli* MFDpir was generously donated by the Fernandez Herrero Lab (National Center for Biotechnology in Madrid). pTOX5 was purchased from AddGene (Watertown, USA). pARO190 was purchased from Cedarlane (Burlington, Canada), and Prerna Singh (PhD. candidate) confirmed its sequence in conjunction with Plasmidsaurus (Oregon, USA). The full plasmid map is shown in Figure 2.

was added to LB, LA, TSB and TSA media to ensure cell growth of the MFDpir donor strain during the conjugation experiment. Carbenicillin (Crb, 100 µg/mL) was used to select for colonies hosting pARO190 recombinants. Gentamicin (Gm, 10-15 µg/mL) was used to select for colonies hosting pTA-Mob. Chloramphenicol (Cm, 100 µg/mL) was used to select for colonies hosting the pTOX5 recombinants.

IPTG (0.5 mM) was added to TSB media to induce mEBPs expression during the NPs production experiment. The chemicals for the LC-MS run are: HPLC-grade H₂O, LC-MS-grade formic acid, acetone and LC-MS-grade methanol were all obtained from Fisher chemical, while HPLC-grade acetonitrile (CAN) was obtained from Sigma-Aldrich.

EBPs modification (mEBPs) and recombinant plasmid construction

Primer design. All primers designed are under 40 nucleotide residues (bases). The G-C content ranges between 50-69 %, except for the bEBPs modification (mEBPs) reverse complement (RC) primers, which are under 60 b due to the His tag. The melting temperatures (T_m) range varies between 53-61 °C. The 3' end had G and C bases added as frequently as possible.

bEBPs. Colony PCR (cPCR) was performed to confirm the presence of bEBPs in the strain of interest, using primers found in Table A1. A *P. laumondii* colony was resuspended in 50 µL of mqH₂O and heated at 95 °C for 5min, then 5 µL of this liquid was used as template, with Phusion DNA polymerase. The resulting PCR products were visualized on a 1% agarose gel. The PCR settings are found in Table 4 (All reagents were from NEB and IDT DNA).

mEBPs amplicons. To implement the EBPs modifications (Table 2), a cPCR (as described above) using *P. laumondii*'s genome as DNA template was performed with the primers from Table 3. The resulting amplicons were then directly used to generate the recombinant plasmids.

Recombinant plasmid. The amplicons (mEBPs) were digested with restriction enzymes using HindIII and KpnI and ligated with T4 DNA ligase to the appropriately- digested pARO190 (except for *glrR*, where HindIII and Sall were used). All reagents used were from New England Biolabs. After an overnight (ON) incubation at 4 °C. The recombinant plasmids mix was chemically transformed into chemically competent cells (CCC) *E. coli* DH5 α , following a protocol from OpenWetWare⁶³ with one correction: the volume of TSS (transformation and storage solution) buffer used was 3 % of the initial incubation volume.

Blue-White colony screening. Following the chemical transformation, based on a protocol from OpenWetWare⁶⁴ with adjustments including incubating for 45 s at 42 °C for heat shock and 2 h at 225 rpm for growth initiation, the transformed cells were then plated on LA/X-gal/IPTG/Crb+ and incubated ON at 37 °C. Identification of the of the clones with the desired recombinant plasmids was achieved through the blue-white screening. Three white colonies per mEBP were incubated in LB/Crb+ ON at 225 rpm and 37 °C, then stored at -80 °C in 20 % glycerol. The recombinant plasmids were extracted and confirmed by sequence analysis (Genome Quebec Innovation Center/McGill University).

Table 2. Modified bEBPs used in this work.

Name	Region conserved	Source
DctD ₍₁₄₁₋₃₉₄₎	Start from codon 141 to 394	Gen9
PspF-M	1 st aa modified LEU (TTG) to MET (ATG)	This work
PLU_RS06090 _(Δ2-304)	Start from codon 305 to stop codon	This work
PLU_RS06090 _(Δ2-320)	Start from codon 321 to stop codon	This work
GlrR _(Δ2-122)	Start from codon 123 to stop codon	This work
GlrR _(Δ2-131)	Start from codon 132 to stop codon	This work
TyrR _(Δ2-123)	Start from codon 124 to stop codon	This work
TyrR _(Δ2-200)	Start from codon 201 to stop codon	This work
PrpR _(Δ2-208)	Start from codon 209 to stop codon	This work

For DctD₍₁₄₁₋₃₉₄₎ only the C domains was used, with the sequence derived from *S. meliloti*. For the rest of the modified bEBPs the R domain was deleted. These sequences were obtained from *P. laumondii* (DSM15139) via cPCR.

the palette was resuspended with TSB/DAP. The samples were mixed in a 3:1 ratio (recipient to donor), plated as a small circle on a TSA/DAP and incubated ON at 30 °C. Day2, cells were collected from the ON plate, resuspended in TSB (DAP removal selects against the donor strain, *E. coli* MFDpir) then plated on TSA/Crb+ and incubated 48-72 h at 30 °C. Three colonies per mEBP variant were incubated in TSB/Crb+ ON at 225 rpm and 30 °C, then stored at -80 °C in 20 % glycerol. The presence of the strain and plasmid was confirmed via cPCR (as described above), using M13 primers to verify the presence of pARO190, and primers targeted to *pir* and *pspF* to confirm the strain as *E. coli* or *P. laumondii*, respectively (Table 5).

Table 5. Primers used to confirm strains or plasmid identity.

Primers	Sequences
FW- <i>pir</i>	TCACACCCTGGCTCAACTTC
RC- <i>pir</i>	TTTGGGAGGTACGGTTTCATCA
FW- <i>pspF</i>	TGGGTGAAGCAAACAGCTTTC
RC- <i>pspF</i>	AGTCGTAGTTTCTCTGCTGCTT
FW-M13	GTAAAACGACGGCCAGT
RC-M13	CAGGAAACAGCTATGAC

All primers were ordered from IDT DNA. Abbreviations, FW: forward primer and RC: reverse complement primer

NP production, extraction, and analysis protocols

NP production. A 4 day growth protocol from Maythem Ali was adjusted. An overnight culture of *P. laumondii* carrying the plasmid of interest was diluted 100x in TSB/Cr⁺. IPTG was then added to a final concentration of 0.5 mM, alongside 200 µL of sterile Amberlite XAD-16 beads per 10 mL of sample. Cells were then incubated at 30 °C, 250 rpm for 4 days. A sample containing all the elements except the recipient strain was used as a negative control. Each strain was tested in triplicate.

Extraction. After the 4 day incubation, the samples were centrifuged at 4 °C, 4 krpm for 5 min. The pellets were collected and resuspended with cold TBS, then centrifuged for 1min at 13.3 krpm.

The washes were repeated 3 times. The pellets were resuspended with a 1:1 MeOH to Acetone mix; incubated at 30 °C, 250 rpm for 15 min; centrifuged 1 min at 13 krpm then the supernatants were collected and speed vacuumed until obtaining pellets. Samples were stored at -80 °C.

Sample preparation for LC-MS. The samples' pellets were resuspended using MeOH (with leucine enkephalin acetate as an internal standard at 18 mM); sonicated for 10 min, then centrifuged 1 min at 13 krpm. Supernatants were then transferred to clear vials. Aliquots of 20 µL of each sample were pooled for quality control testing and a 1:1 solution of methanol: acetone was used as a blank. All samples were stored in the dark at room temperature until the LC-MS run.

LC-MS run. LC-MS/MS analyses were performed on an Agilent 1100 LC system coupled to a Thermo LTQ Orbitrap Velos mass spectrometer equipped with a heated electrospray ion source at positive mode. The column used was a CORTECS ® T3 2.7 µm, 2.1x100mm column at a flow rate of 0.3 ml min⁻¹ with a 10 µl injection volume. The compounds were eluted using a 34 min gradient at a flow rate of 300 µL/min with mobile phase A (water containing 0.1 % FA) and B (ACN containing 0.1 % FA). The gradient started at 5 % B and held for 1 min, linear gradients were achieved to 95 % B at 20 min (Table 6). The mobile phase was held at 95 % B for 7 min, then reduced to 5 % B for 7 min. A full MS spectrum (m/z 150-2000) was acquired in the Orbitrap at a resolution of 100000, with the five most abundant singly and doubly charged ions each second selected for MS/MS fragmentation in the linear trap, with the option of dynamic exclusion. Compound fragmentation was performed using a collision induced dissociation at normalized collision energy of 35 % with activation time of 10 ms. The spectra were internally calibrated using diisooctyl phthalate (m/z 391.2843 Da) as a lock mass.

Data analysis: Compound discoverer 3.3 and Thermo XCalibur Qual Browser were used to analyse the data collected from the LC-MS run. The data were internally adjusted using a

compound present in the background as a reference (m/z 245.1286 Da) to account for a shift in mass, as determined by the quality control observation. This was followed by filters based on a mass tolerance of 5ppm at MS1 and the presence of an MS2 fragmentation profile with a mass tolerance of 0.6Da.

Table 6. PCR cycle used in this study.

Time (min)	A (%)	B (%)	Flow (mL/min)	Max. Pressure Limit (bar)
0.00	95.0	5.0	0.300	340.00
1.00	95.0	5.0	0.300	340.00
20	5.0	95.0	0.300	340.00
27.00	5.0	95.0	0.300	340.00
27.00	95.0	5.0	0.300	340.00
34.00	95.0	5.0	0.300	340.00

Knockout Cassettes

Knockout cassettes for five genes of interest in *P. laumondii* were designed and ordered from IDT DNA, including *rpoN* (Table A2). They were then cloned independently into pTOX5 (Figure A1 and Table A3) using T4 DNA ligase at restriction sites EcoRV and PacI. All reagents used were from New England Biolabs.

RESULTS

Bioinformatic analysis

1. Strain selection.

To evaluate the best strain for this study, Dr. Brandon Findlay compared 13 different families of *Gammaproteobacteria*. The genomes were obtained from NCBI and analysed using antiSMASH³⁶ under default settings. Several strains of *Streptomyces* spp. were added for scale (Figure 3). Most families analysed had less than 15 BGCs, while only 4 families were found to have strains with more than 19 BGCs. Among them, the *Photorhabdus* spp. (Figure 3, red box) showed great potential. Due to it being a type strain and the presence of 22 newly identified BGCs (Table A4), the *Photorhabdus laumondii* DSM 15139 strain was selected to serve as the model organism in this work.

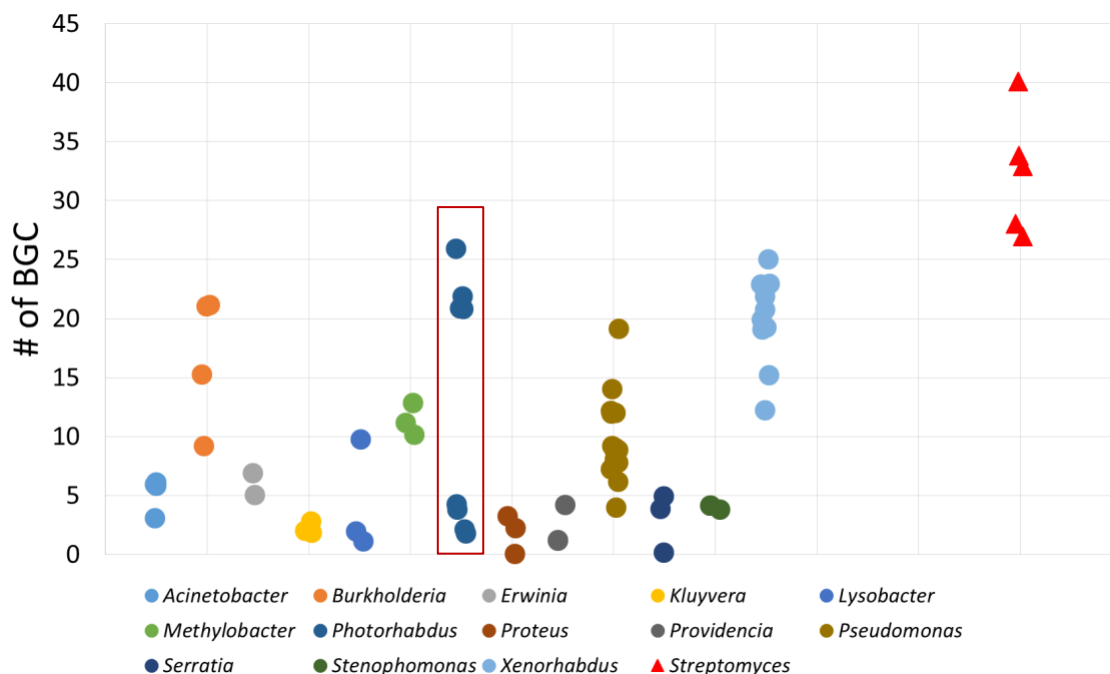


Figure 3. BGCs' distribution amongst *Gammaproteobacterial* families.

Photorhabdus spp. was selected (red box) as a model Gram-negative entomopathogenic bacterium due to its potential for BGCs count. *Streptomyces* spp. was added for scale. Unpublished data. Figure made by Dr. Brandon Findlay.

2. bEBPs identified in *P. laumondii* TTO1.

To identify the σ^{54} -bEBPs present in *P. laumondii* TTO1, we used as a template the *Sinorhizobium meliloti* DctD core (C) domain (DctD₍₁₄₁₋₃₉₄₎), containing the σ^{54} binding domain³⁵, obtained from Gen9. The NCBI protein-protein BLAST (blastp) search was conducted under default settings, revealing a total of six bEBPs with E values below a cut-off of 1e-10: GlnR (3e-73), GlnG (3e-61), TyrR (3e-57), PspF (1e-56), PrpR (3e-52) and PLU_RS06090 (2e-59) (Table 7 and Figure A2).

Table 7. Identified σ^{54} -dependent bEBPs in *P. laumondii* TTO1.

Genes	Description	E value	Old locus tag	Accession
<i>glrR</i>	two-component system response regulator	3 e-73	plu3311	WP_011147503.1
<i>glnG</i>	Nitrogen regulatory protein RN(I)	3 e-61	plu0235	WP_011144634.1
<i>tyrR</i>	Transcriptional regulatory protein TyrR	3 e-57	plu2580	WP_011146802.1
<i>pspF</i>	Phage shock protein operon transcriptional activator	1 e-56	plu2586	WP_011146808.1
<i>prpR</i>	Propionate catabolism operon regulatory protein PrpR	3 e-52	plu3543	WP_011147723.1
<i>PLU_RS06090</i>	NRPS – Unknown	2 e-59	plu1233	WP_011145558.1

Using NCBI BLASTp and NCBI database. bEBPs identified in *P. laumondii* TTO1 using σ^{54} binding sequence (core domain) from *S. meliloti* DctD bEBP as a template.

Further enquiry revealed that among these six putative bEBPs, the GAFTGA sequence motif was present in four, namely GlnR, GlnG, PspF and PLU_RS06090. This motif is necessary for the bEBP- σ^{54} interaction and thus the activation of the RNAP- σ^{54} holoenzyme³¹. Despite lacking this motif, TyrR and PrpR were included in this study due to their high homology to DctD C domain, as indicated by their respective E value 3e-57 and 3e-52, aiming to assess their effect on NP biosynthesis in *P. laumondii*.

Generating variants

The presence of all of the bEBPs in *P. laumondii* TTO1, save for *glnG*, was then verified by cPCR in *P. laumondii* TTO1 using primers from Table A1. These five bEBPs were then modified by cPCR using primers from Table 3 to remove the leading regulatory (R) domain as indicated in Table 2, and referred to hereafter as mEBPs. Different deletion ranges were explored for some bEBPs based on a UniProt review of their R domain (Table A5). Those with unidentified R domains like PrpR had all the region preceding the core domain deleted, whereas those with known regulatory elements underwent two deletions: one removing only the regulatory elements, and the second deleting the entire region before the core domain. For PLU_RS06090, GlrR and TyrR, two deletions were obtained for each: PLU_RS06090_(Δ2-304) and PLU_RS06090_(Δ2-320); GlrR_(Δ2-122) and GlrR_(Δ2-131); as well as TyrR_(Δ2-123) and TyrR_(Δ2-200). For PrpR as mentioned only one deletion was obtained PrpR_(Δ2-208). As for PspF, since it did not contain an R domain, a modification to its first codon (TTG, Leu) to a start codon (ATG, Met) was the only change required. These mEBPs including DctD₍₁₄₁₋₃₉₄₎, were then ligated into pARO190, identified in *Escherichia coli* DH5_α using blue-white screening, sequenced to confirm the modifications, and then chemically transformed into donor strain *E. coli* MFDpir. With the exception of PrpR_(Δ2-208), all of these mEBPs were then successfully conjugated into *P. laumondii* TTO1, thus generating the different variants named after the mEBP they carry.

Before successfully introducing the recombinant plasmids in *P. laumondii* TTO1, multiple protocols were attempted, over 100 chemical transformations, 30 electroporation and 27 conjugations, all yielding no results. The first successful conjugation was that of TyrR_(Δ2-200) using an optimized protocol from the Bode lab. The presence of the different mEBPs in *P. laumondii* TTO1 was confirmed via cPCR using primers from Table 5, as demonstrated in Figure 4.

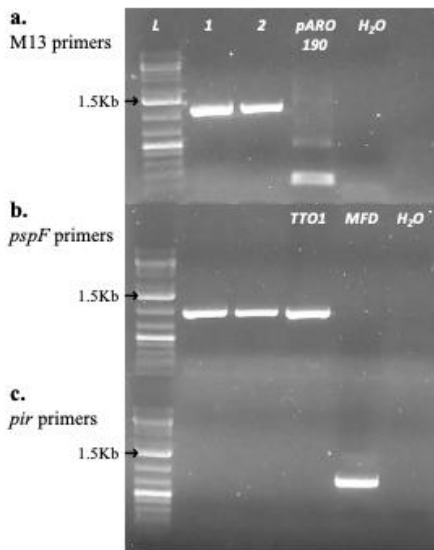


Figure 4. cPCR confirmation of pARO190-tyrR_(Δ2-123) conjugation. For each gel: column 1 is the ladder (L); column 2 is cPCR product from TyrR_(Δ2-123)Y variant (1); column 3 is cPCR product from TyrR_(Δ2-123)B variant (2); all the remaining columns are identified with the different controls. **a.** Verifying plasmid presence using M13 primers; **b.** Validating *P. laumondii* TTO1 strain presence using pspF primers; **c.** Confirming MFD(pir⁺) strain absence using pir primers. The verification primer sequences are found in Table 5.

Effect of mEBPs on Cell Growth

Upon the successful generation of the variants containing the different mEBPs, triplicates of each variant were produced, and the three main phenotypes of color, shape, and growth rate of each sample were recorded (Table 8). Singlicate samples of the media and *P. laumondii* TTO1 strain were assessed as controls.

All variants exhibited normal growth, with the exception of TyrR_(Δ2-200). This variant had notably slower growth than the other samples, forming very small, bright yellow colonies. The variants PLU_RS06090_(Δ2-320), GlrR_(Δ2-131) and TyrR_(Δ2-123) grew at normal rates, but formed a mixture of beige and yellow-pigmented colonies, suggesting heterogeneous gene expression. To distinguish between the two different colony types, subgrouping by letters was implemented, those with yellow or beige pigmentation were designated Y or B, respectively (Table 8). The complete observations on the samples phenotypes and metabolites extracts can be found in Table A6.

Table 8. Variants phenotypic categorization.

Categories	Yellow colonies	Beige colonies
Round shaped and regular growth	PLU_RS06090(Δ 2-320)Y; GlrR (Δ 2-131)Y; TyrR(Δ 2-123)Y	TTO1 WT; pARO190; DctD ₍₁₄₁₋₃₉₄₎ ; PspF-M; PLU_RS06090(Δ 2-304); PLU_RS06090(Δ 2-320)B; GlrR(Δ 2-122); GlrR(Δ 2-131)B; TyrR(Δ 2-123)B
Small and slow growth	TyrR(Δ 2-200)	-

Each variant was named based on the mEBP it carries. Y (yellow) and B (beige) reflect the subgrouping for the same mEBP.

Assessing the effect of DctD₍₁₄₁₋₃₉₄₎ on NP biosynthesis

1. Effect on metabolite expression.

To be able to analyse the effect that the different mEBPs have on *P. laumondii* TTO1 NP expression, this approach had to be tested using the well-studied bEBP, DctD. To document the effect of DctD₍₁₄₁₋₃₉₄₎, an LC-MS analysis was performed with the help of Heng Jiang, a mass spectrometry specialist at Concordia University. The prepared LC-MS samples were run in positive mode and a chromatogram, truncated due to background noise (Figure A2), showing the DctD₍₁₄₁₋₃₉₄₎ variant metabolite profile (blue) was obtained as seen in Figure 5. Media, *P. laumondii* TTO1 and *P. laumondii*-pARO190 samples were used as controls.

In the *P. laumondii* TTO1 strain chromatogram (gray), metabolites expression was located between 7 and 11 min, with moderate peak intensity. For the *P. laumondii*-pARO190 strain chromatogram (red), we noted significant new metabolite expression in the 11-19 min window. Sequencing of the pARO190 showed no unexpected genetic material present (Figure 2), suggesting that pARO190 alone is sufficient to induce a wide range of metabolite biosynthesis. Analysis of the DctD₍₁₄₁₋₃₉₄₎ variant revealed an increase in peaks intensity, as well as the presence of new peaks when compared to *P. laumondii*-pARO190 (asterisks). This indicates an activation in metabolite expression.

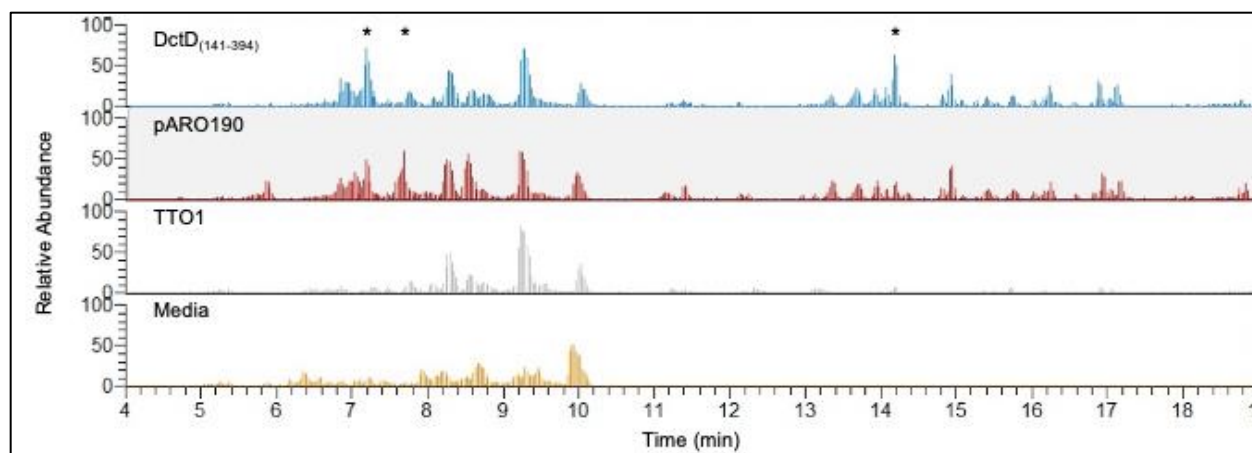


Figure 5. Effect of DctD₍₁₄₁₋₃₉₄₎ on metabolites expression in *P. laumondii* TTO1.

The chromatograms Y axis indicates the metabolites relative abundance (PH) at a scale of **8.00 E8**. The X axis indicates the elution time in minutes of the different metabolites, between 4-19 min. Asterisks denote new and high intensity peaks. Data analysed on Thermo XCalibur Qual Browser.

2. Effect on NP expression.

a. Compound analysed.

To test the induction of NP expression in *P. laumondii*, six known compounds were selected to be identified and assessed (Table 9). Two of these compounds, mevalagmapeptide A and gameXpeptide A, have proposed structures but have yet to be fully characterized²⁴. The remaining four compounds were selected based on the fact that their structure and function are well-documented.

Table 9. Compounds to be analysed in this study.

Compounds	Abbreviations	Functions
Mevalagmapeptide A	MVAP-A	Unknown biological activity. ²¹
Phurealipid A	PL-A	Act as an immunosuppressant and inhibits the development of the insect larva. ³⁸
Photopyrone D	PPY-D	Cell to cell communication (Quorum sensing) and regulation of NPs production. ^{39,40}
Isopropylstilbene	IPS	Has insecticidal and antimicrobial activities. ^{41,42}
Anthraquinone 270	AQ-270	Is a pigment with some antimicrobial activity and act as a bird and insect deterrent. ⁷
GameXpeptide A	GXP-A	Unknown biological activity. Detected only inside the host insect. ^{41,43}

Each of these compounds was identified by MS/MS in the LC-MS data using Compound Discoverer 3.3. Three out of the six compounds exhibited multiple peaks with the same MS reading, which were spread across the range of elution time, suggesting the presence of isoforms (Figure 6-8). A single peak per compound was selected for further analysis based on the presence of an MS/MS data and clear fragmentation patterns to identify the structure.

Phurialipid A (PL-A.) has a molecular weight of 228.2202 Da and m/z 229.2274 $[M+H]^+$. We can observe from the chromatogram in Figure 6A that a compound with a corresponding m/z has eluted at five different time points. The compound identity at position 4 (RT 15.2 min) was confirmed based on the fragments observed on the MS/MS spectrum (Figure 6B). The m/z of the two main fragments are 172.18 and 186.20, which correspond to $[C_{13}H_{29}N_2O]^+ - [C_4H_9]$ and $[C_{13}H_{29}N_2O]^+ - [C_3H_7]$ respectively.

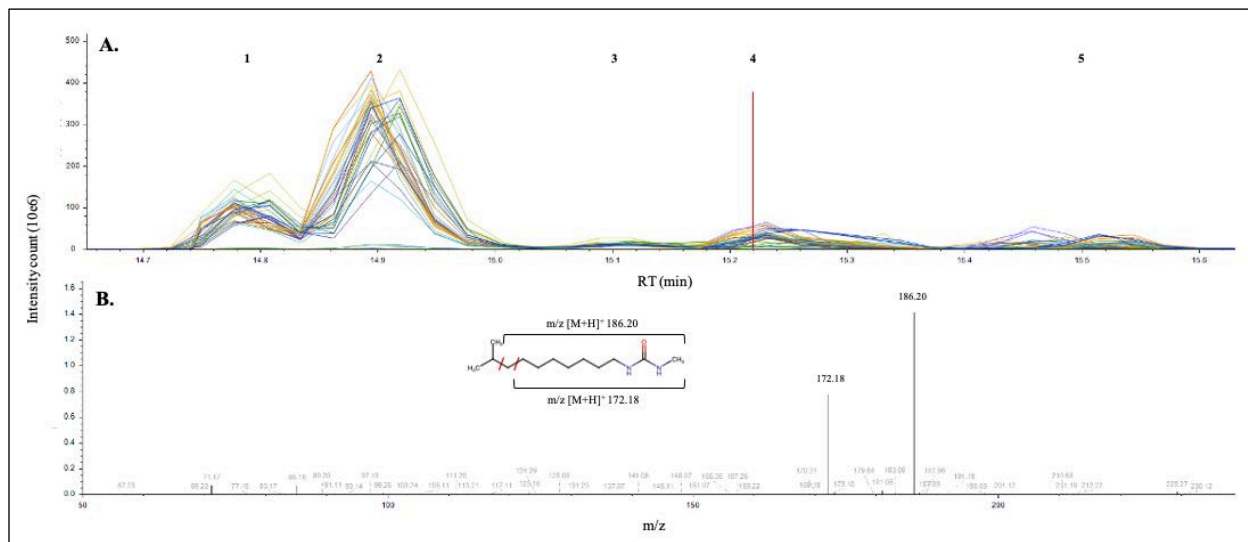


Figure 6. PL-A identification.

The Y axis represent the intensity count. **A.** This chromatogram reflects the data from all the variants in triplicates (39 samples). Peaks 1-5 represent the different isoforms. The red line indicates the peaks for which MS/MS fragmentation analysis was made. X axis is retention time (RT, min). **B.** the MS/MS spectrum shows the fragments obtained at RT 15.22 min. X axis is m/z . The structure of the compound with a proposed cut position for the analyzed fragments, m/z 172.18 and 186.20. LC-MS data analysed on Compound Discoverer 3.3.

Anthraquinone 270 (AQ-270) has a molecular weight of 270.0528Da and m/z 271.0601 $[M+H]^+$. We can observe from the chromatogram in Figure 7A that a compound with a corresponding m/z has eluted at four different time points. The compound identity at position 1 (RT 11.0 min) was confirmed through the analysis of two fragments observed on MS/MS fragmentation spectrum. They had m/z of 241.15 and 256.14 which correspond to $[C_{15}H_{11}O_5]^+ - [OCH_3]$ and $[C_{15}H_{11}O_5]^+ - [CH_3]$ respectively (Figure 7B).

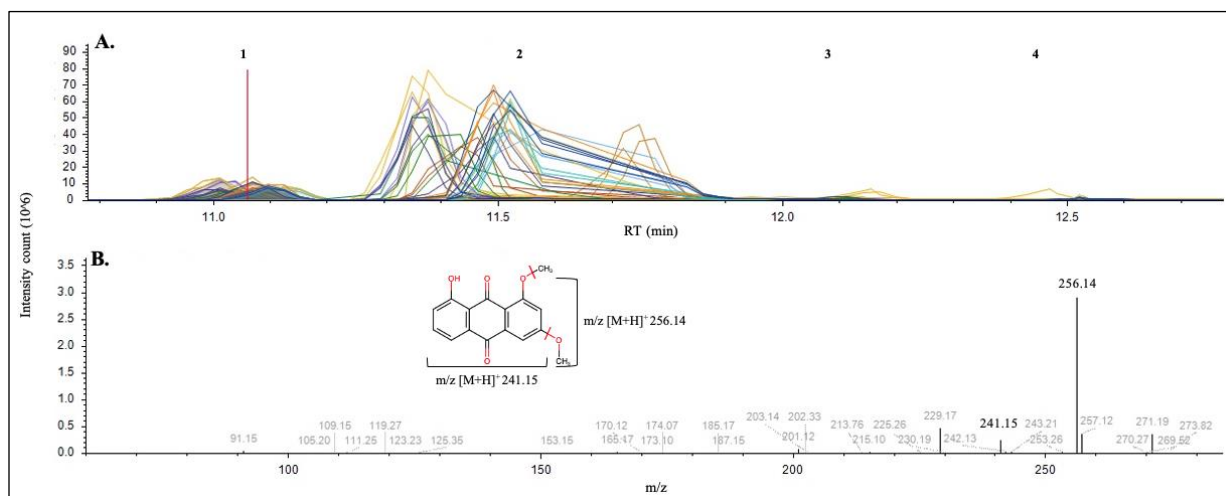


Figure 7. AQ-270 identification.

The Y axis represent the intensity count. **A.** This chromatogram reflects the data from all the variants in triplicates (39 samples). Peaks 1-4 represent the different isoforms. The red line indicates the peaks for which the MS/MS fragmentation analysis was made. X axis is retention time (RT, min). **B.** the MS/MS spectrum shows the fragments obtained at RT 11.0 min. X axis is m/z . The structure of the compound with a proposed cut position for the analyzed fragments, m/z 241.15 and 256.14. LC-MS data analysed on Compound Discoverer 3.3.

Photopyrone D (PPY-D.) has a molecular weight of 294.2195 Da and m/z 295.2268 $[M+H]^+$. We can observe from the chromatogram in Figure 8A that a compound with a corresponding m/z has eluted at five different time points. The compound identity at position 3 (RT 17.0 min) was confirmed through the analysis of two fragments observed on MS/MS fragmentation spectrum. They had m/z of 237.8 and 253.2 which correspond to $[C_{18}H_{31}O_3]^+ - [C_4H_9]$ and $[C_{18}H_{31}O_3]^+ - [C_3H_6]$ respectively (Figure 8B).

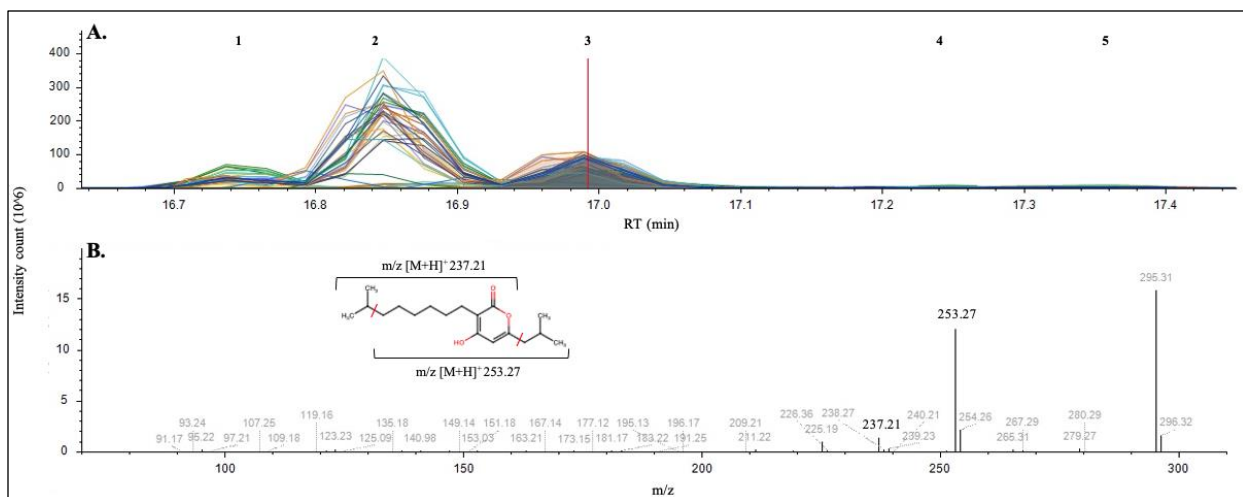


Figure 8. PPY-D identification.

The Y axis represent the intensity count. **A.** This chromatogram reflects the data from all the variants in triplicates (39 samples). Peaks 1-5 represent the different isoforms. The red line indicates the peaks for which the MS/MS fragmentation analysis was made. X axis is retention time (RT, min). **B.** the MS/MS spectrum shows the fragments obtained at RT 17.0 min. X axis is m/z. The structure of the compound with a proposed cut position for the analyzed fragments, m/z 237.21 and 253.27. LC-MS data analysed on Compound Discoverer 3.3.

GameXpeptide A (GXP-A) has a molecular weight of 585.3890 Da and m/z 586.3963 [M+H]⁺.

We can observe from the chromatogram in Figure 9A that a compound with a corresponding m/z has eluted once. The compound identity at position RT 15.7 min was confirmed through the analysis of two fragments observed on MS/MS fragmentation spectrum. They had m/z of 473.4 and 558.4 which correspond to [C₃₂H₅₂N₅O₅]⁺-2[C₄H₉] and [C₃₂H₅₂N₅O₅]⁺-2[CH₂] respectively (Figure 9B).

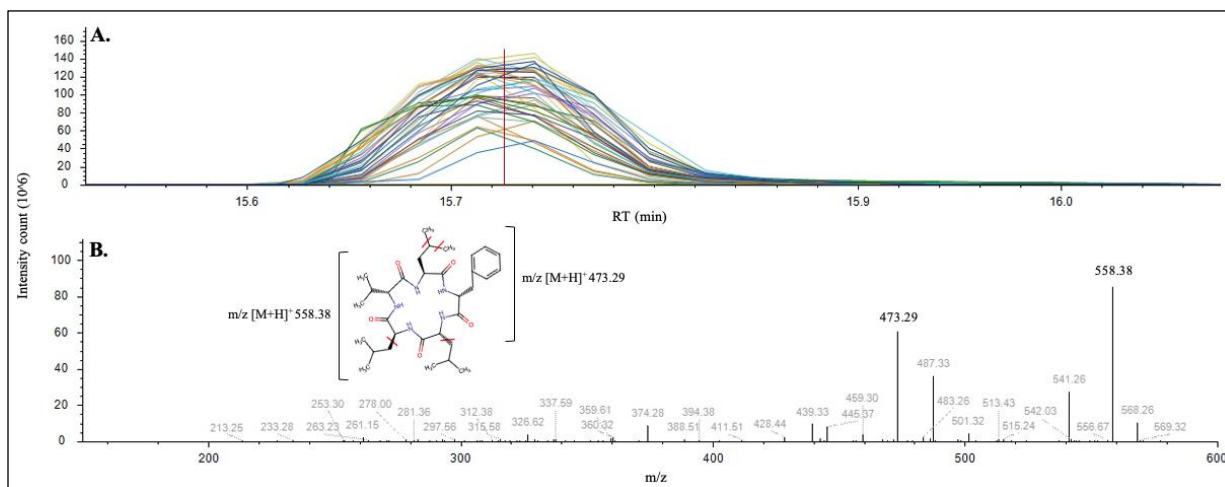


Figure 9. GXP-A identification.

The Y axis represent the intensity count. **A.** This chromatogram reflects the data from all the variants in triplicates (39 samples). The red line indicates the peaks for which the MS/MS fragmentation analysis was made. X axis is retention time (RT, min). **B.** the MS/MS spectrum shows the fragments obtained at RT 15.7 min. X axis is m/z. The structure of the compound with a proposed cut position for the analyzed fragments, m/z 473.29 and 558.38. LC-MS data analysed on Compound Discoverer 3.3.

Isopropylstilbene (IPS) has a molecular weight of 254.1307 Da and m/z 255.1379 [M+H]⁺. We can observe from the chromatogram in Figure 10A that a compound with a corresponding m/z has eluted once. The compound identity at position RT 13.9 min was confirmed through the analysis of the main fragment observed on MS/MS fragmentation spectrum. It had m/z of 213.43 which corresponds to [C₁₇H₁₉O₂]⁺-[C₃H₆] (Figure 10B).

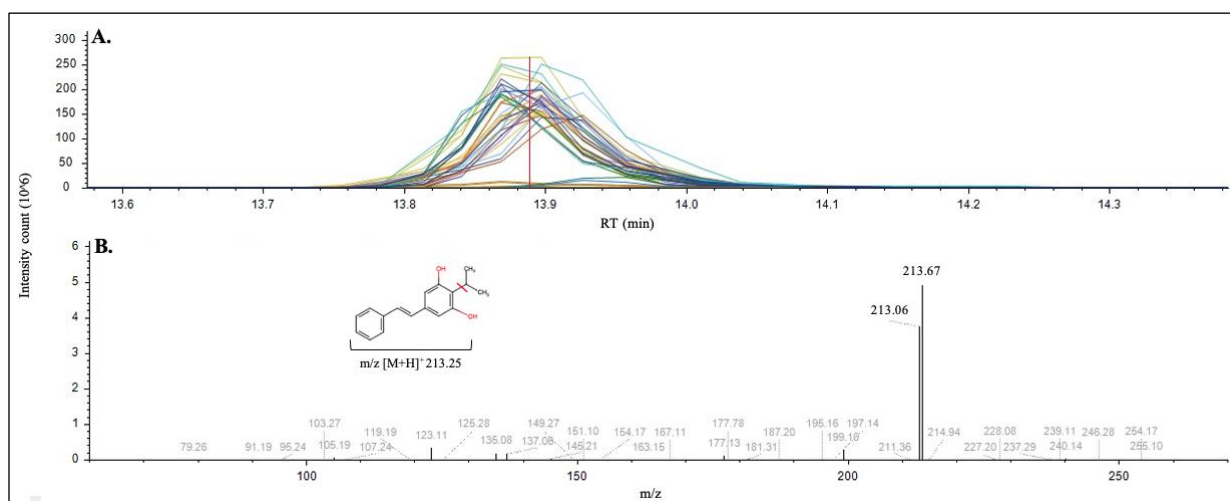


Figure 10. IPS identification.

The Y axis represent the intensity count. **A.** This chromatogram reflects the data from all the variants in triplicates (39 samples). The red line indicates the peaks for which the MS/MS fragmentation analysis was made. X axis is retention time (RT, min). **B.** the MS/MS spectrum shows the fragments obtained at RT 13.9 min. X axis is m/z. The structure of the compound with a proposed cut position for the analyzed fragment, m/z 213.67. LC-MS data analysed on Compound Discoverer 3.3.

Mevalgmapeptide A (MVAP-A) has a molecular weight of 667.5109 Da and m/z 334.7627 [M+2H]²⁺. We can observe from the chromatogram in Figure 11A that a compound with a corresponding m/z has eluted once. The MS/MS spectrum at position RT 7.2 min (Figure 11B) show two main fragments with m/z 326.32 and 343.34. These two fragments correspond to the compound being split in two (343.3 + 326.3 = 2*334.8) consistent with MVAP-A.

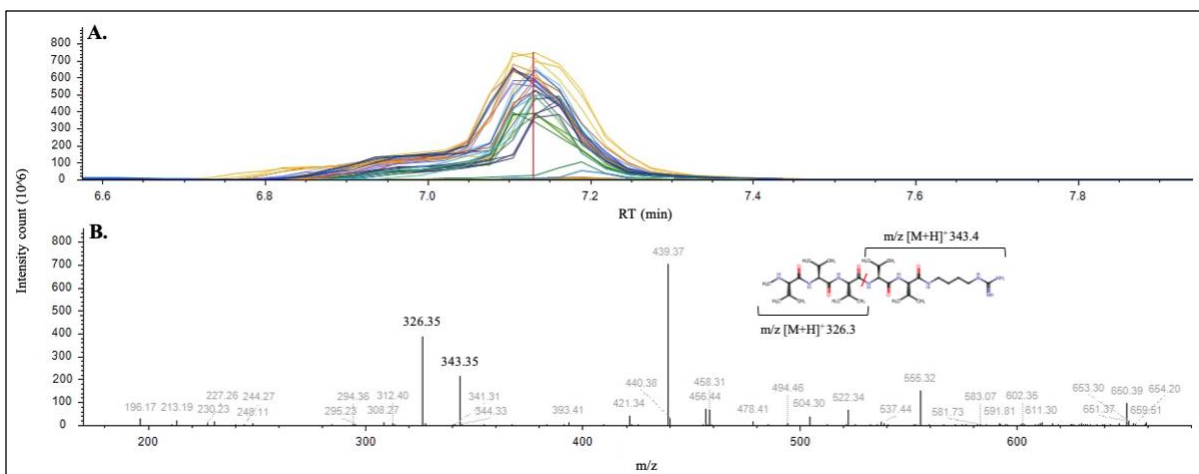


Figure 11. MVAP-A identification.

The Y axis represent the intensity count. **A.** This chromatogram reflects the data from all the variants in triplicates (39 samples). The red line indicates the peaks for which the MS/MS fragmentation analysis was made. X axis is retention time (RT, min). **B.** the MS/MS spectrum shows the fragments obtained at RT 7.2 min. X axis is m/z. The structure of the compound with a proposed cut position for the analyzed fragments, m/z 326.35 and 343.35. LC-MS data analysed on Compound Discoverer 3.3.

b. Compound expression.

The data collected for each of the six compounds from the DctD₍₁₄₁₋₃₉₄₎ variant and *P. laumondii*-pARO190 was derived from three biological replicates, while those from *P. laumondii* TTO1 and the media were analyzed in singlicate. The results of this analysis, which were normalized to *P. laumondii*-pARO190, can be seen in Figure 12. As expected, the media sample showed no significant presence of the compounds analysed, with all values below the detection limit, except for GXP-A that was detected at 0.14 %-fold change. The *P. laumondii* TTO1 strain showed readings that were systematically below those of *P. laumondii*-pARO190, indicating that the presence of pARO190 induced NP biosynthesis. In the presence of DctD₍₁₄₁₋₃₉₄₎, 5 of the 6 compounds showed a statistically significant increase relative to the empty vector, with the highest expression (320%) for PL-A. No statistically significant difference was observed for the production of IPS. All raw data linked to compound production levels per variant is found in Table A7.

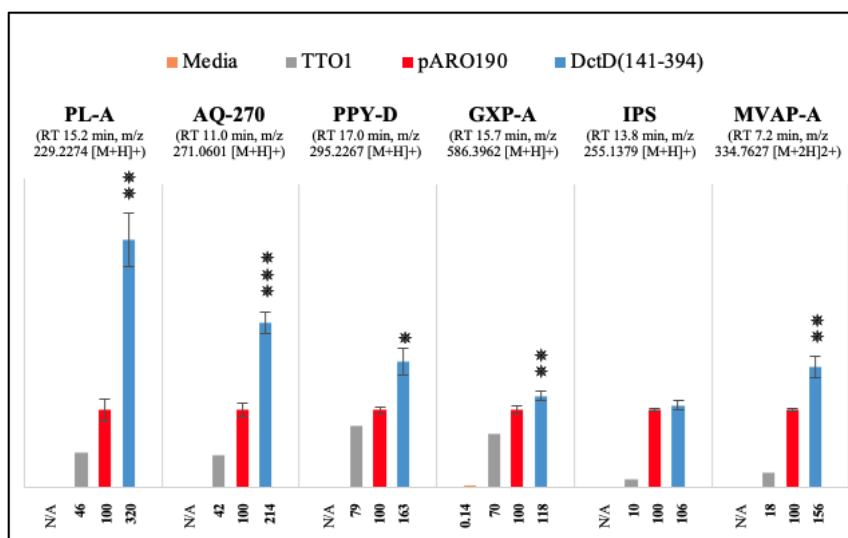


Figure 12. Effect of DctD₍₁₄₁₋₃₉₄₎ on NPs expression levels in *P. laumondii* TTO1.

The media, TTO1 and pARO190 samples are used as controls to evaluate the DctD₍₁₄₁₋₃₉₄₎ effects. *P. laumondii*-pARO190 expression levels are considered the normal levels in this study. The Y axis indicates the % fold change relative to the *P. laumondii*-pARO190 levels and they are displayed on the X axis per sample. The asterisks signify that the values calculated using the student t-test, were statistically significant ($p \leq 0.05$). The % fold change was computed by averaging the triplicate values of relative abundance for each variant (Table A7). The compounds full name can be found in the List of Abbreviations.

Assessing the effect of mEBPs on NP biosynthesis

1. Effect on metabolite expression.

With the effect of DctD₍₁₄₁₋₃₉₄₎ established, we turn to the mEBPs. Each mEBP was assessed in triplicate, with Thermo XCalibur Qual Browser once more used to establish the metabolite expression profile (Figure 13). Each variant shows a unique metabolite profile, with different relative abundance levels even within the same subgroup. While greater peak intensity was observed following mEBP expression in general, PLU_RS06090_(Δ2-304), TyrR_(Δ2-123)B and TyrR_(Δ2-200) all show a notable reduction in signal intensity. TyrR_(Δ2-200) in particular nearly completely repressed expression, giving results most similar to the media control (Figure 5).

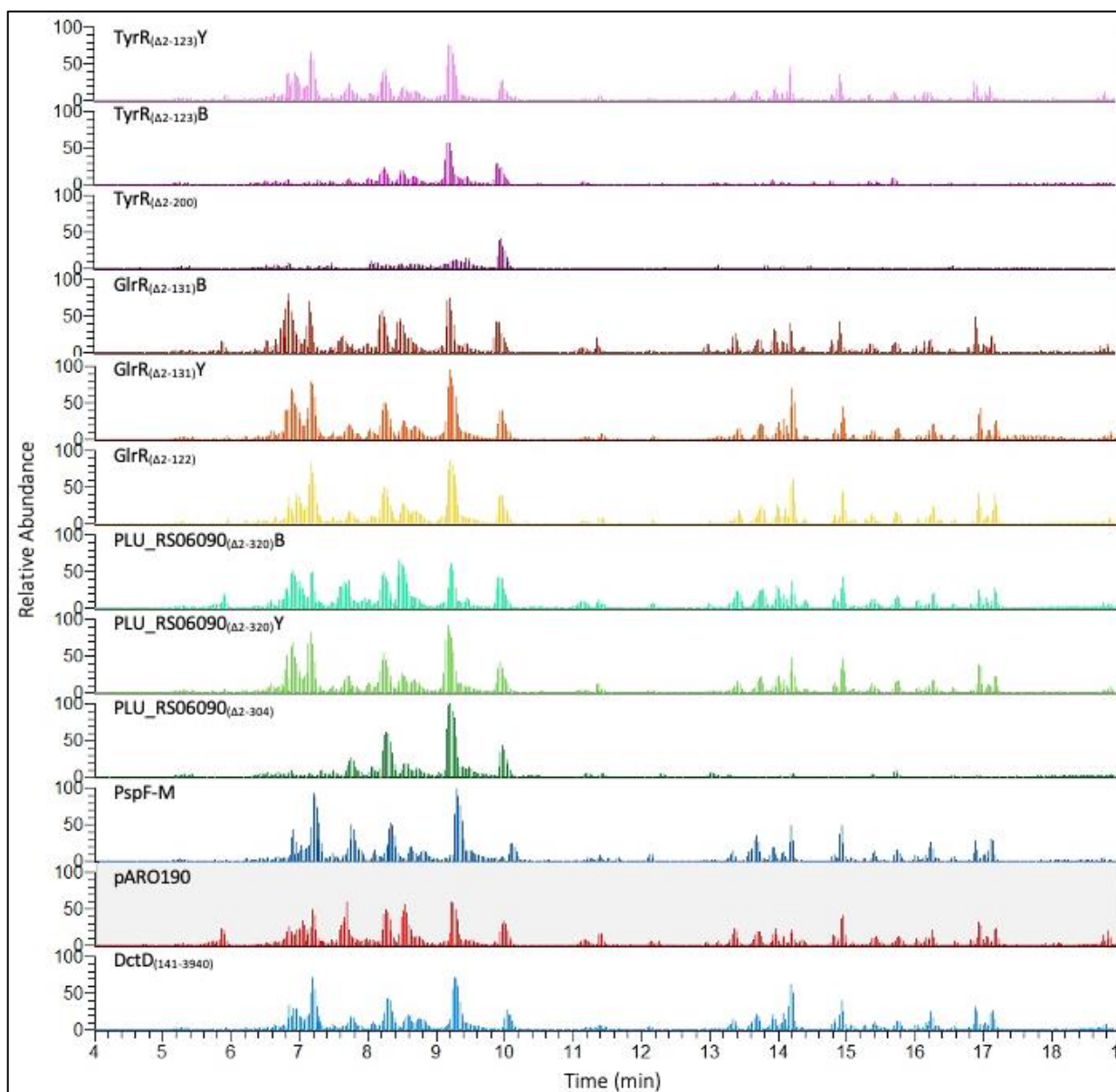


Figure 13. Effects of mEBPs on metabolite expression in *P. laumondii* TTO1.

The chromatograms Y axis indicates the metabolites relative abundance (PH) at a scale of 8.00×10^8 . The X axis indicates the elution time in minutes of the different metabolites, between 4-19 min. The *P. laumondii*-pARO190 (red) and DctD₍₁₄₁₋₃₉₄₎ (light blue) variant are used as controls to evaluate the mEBPs effects. One chromatogram figure per variant triplicate was selected for display. LC-MS data analysed on Thermo XCalibur Qual Browser.

2. Effect on NP expression.

As previously observed, DctD₍₁₄₁₋₃₉₄₎ has an activating effect on the expression of all six compounds analysed. By using the DctD₍₁₄₁₋₃₉₄₎ variant and *P. laumondii*-pARO190 as scaling controls, representing the state of activated and basal levels of expression respectively, we are able to compare, contrast and determine the effect that each bEBP has on the expression of these compounds. The data shown in Figure 14, was compiled from three replicates which was normalized to *P. laumondii*-pARO190.

As anticipated from the metabolite profile, the TyrR_(Δ2-200) variant showed no compound expression. All traces of the compounds are below the detectable limits of the LC-MS device. These results indicate a clear repressive function of the TyrR_(Δ2-200) mEBP in the *P. laumondii* TTO1 strain. On the other hand, TyrR_(Δ2-123)Y and B showed contradictory readings of activation and repression respectively (Figure 14). Due to this unexplained inconsistency, and the lack of a GAFTGA sequence, both TyrR_(Δ2-123) variants were excluded pending further analysis.

In general, all GlrR variants activated NP biosynthesis above that of *P. laumondii*-pARO190, and in some cases higher than those of DctD₍₁₄₁₋₃₉₄₎. The results obtained for the two GlrR_(Δ2-131) variants showed the same general activation trend but varied greatly in the levels of compound expression. These variations require further examination to determine the cause(s), for this reason they were not be further analysed. In the case of GlrR_(Δ2-122) variant, we can clearly confirm an activating function since 5 of the 6 compounds are statistically significantly higher than *P. laumondii*-pARO190 values (black asterisk). In the case of GPX-A it was above that of DctD₍₁₄₁₋₃₉₄₎ (red asterisk), confirming that GlrR bEBP has a general activating effect on NP expression in the TTO1 strain.

For the PLU_RS06090 variants, the results obtained from the two PLU_RS06090 deletions are opposite. For PLU_RS06090(Δ 2-304) variant, all the results obtained are below those of *P. laumondii*-pARO190 but above those observed for TyrR(Δ 2-200), indicating a more moderate repressive function. For the PLU_RS06090(Δ 2-320) variants, although their compound expression levels show great variability, they exhibited a general activation trend, with values above that of *P. laumondii*-pARO190. These observations seem to indicate that PLU_RS06090 bEBP has two functions. Activation and repression of NP expression in the *P. Laumondii* TTO1 strain seem to depend on the extent of R domain deletion.

For the PspF-M variant, almost all the results obtained are statistically significantly above those of *P. laumondii*-pARO190. Notably, the expression levels of AQ-270, GXP-A and MVAP-A are above those seen in DctD₍₁₄₁₋₃₉₄₎ (red asterisk). These results indicate that PspF bEBP has a clear activating function of NP expression in the TTO1 strain.

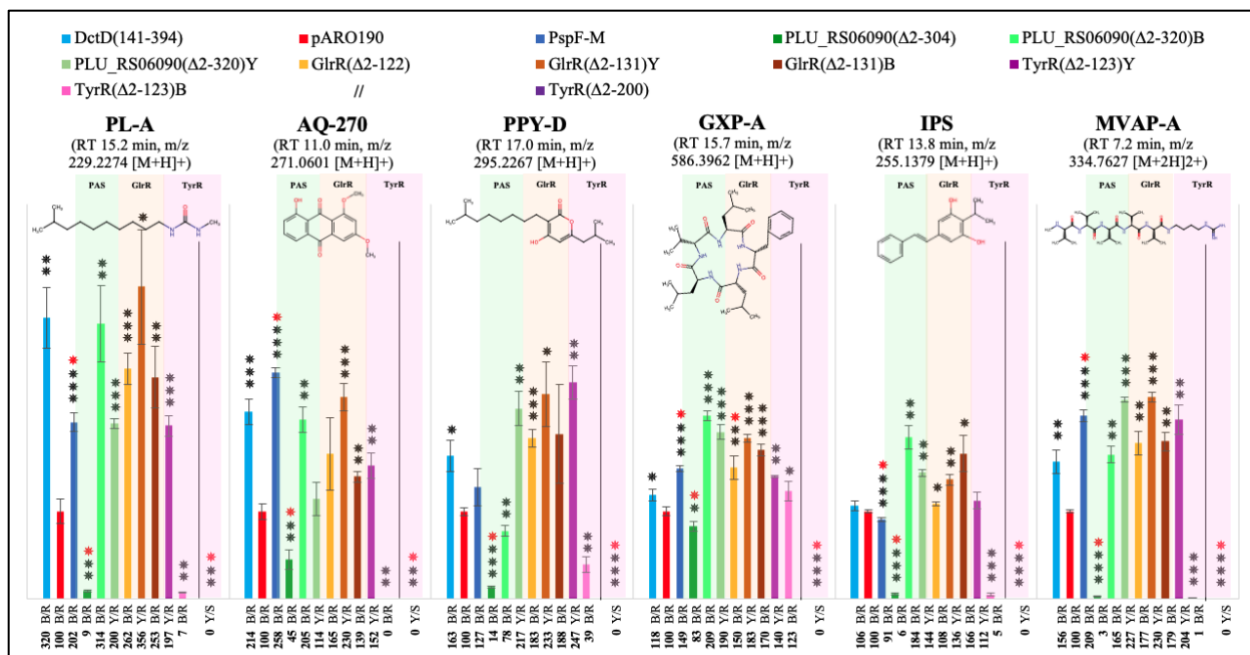


Figure 14. Effect of mEBPs on NP expression levels in *P. laumondii* TTO1.

Each mEBP is represented by a colour category. The *P. laumondii*-pARO190 (red) strain and DctD₍₁₄₁₋₃₉₄₎ (light blue) variant are used as controls to evaluate the different mEBPs effect. In this study, *P. laumondii*-pARO190 expression levels are considered the normal levels and DctD₍₁₄₁₋₃₉₄₎ expression levels represent a state of activation. The Y axis indicates the % fold change relative to the pARO190 levels and they are displayed on the X axis. The phenotypic characteristics of each variant are presented as acronyms on the X axis (B/R: Beige/Regular growth, Y/R: Yellow/Regular growth and Y/S: Yellow/Slow growth). For each compound, the RT, m/z, ionic state, and chemical structure were added. The asterisks signify that the values calculated using the student t-test were statistically significant ($p \leq 0.05$) (black relative to pARO190 and red relative to DctD₍₁₄₁₋₃₉₄₎). The % fold change was computed by averaging the triplicate values of relative abundance for each variant (Table A7). The compounds' full names can be found in the List of Abbreviations.

DISCUSSION

In this study, we aimed to verify if σ^{54} -dependent bEBPs could function as regulators of natural product (NP) biosynthesis, and to test the practicality of inducing said biosynthesis with different bEBPs. As previously stated, bEBPs are proteins that activate RNAP transcription by binding to σ^{54} unit, which subsequently leads to the expression of σ^{54} dependant BGCs.^{30,31}

The model strain for this work, *Photorhabdus laumondii* DSM 15139, contains a large number of BGCs for a *Gammaproteobacteria* (Figure 3). To confirm whether *it* was suitable for testing, we conducted a BLASTp analysis using the core (C) domains DctD (DctD₍₁₄₁₋₃₉₄₎), a well-studied σ^{54} -dependent bEBP. This identified six similar bEBPs (Table 7), four of which contain the σ^{54} -interacting sequence GAFTGA³¹. The other two, TyrR and PrpR, were included in this work to serve as controls for σ^{54} activation and determine their effect on NP expression.

We have modified five of six identified bEBPs to be constitutively active, generally by removing their regulatory (R) domain (Table A5). For three of these mEBPs, two deletions were obtained: the first involved removing the known R elements, and the second involved removing the full sequence before the C domain. Activation of PspF required only the addition of a start codon, while GlnG was not considered in this work.

We constructed recombinant plasmids containing all pARO190-mEBPs, including DctD₍₁₄₁₋₃₉₄₎, and conjugated them in *P. laumondii* TTO1 to generate the different variants. However, pARRO190-PrpR_(Δ 2-208) was an exception, as multiple attempts at conjugation were unsuccessful. As a result, we were unable to proceed with assessing the effect of PrpR bEBPs on NP biosynthesis in *P. laumondii* TTO1. I suspect that PrpR_(Δ 2-208) may have activated the expression of compounds associated with lethal genes⁴⁴, which proved fatal to *P. laumondii*. Basal expression of PrpR_(Δ 2-208), leaked by the *lac* operon⁴⁵ controlling it, could have been sufficient to

kill the strain. This could explain why no conjugants were obtained compared to other mEBPs tested. Further experiments using a tightly controlled promoter like *ara* for instance^{45,46}, are required to verify this hypothesis.

To evaluate the effect of these mEBPs on NP expression, we selected six compounds: MVAP-A, PL-A, AQ-270, IPS, PPY-D and GXP-A. These compounds were chosen to represent the diverse array of NPs produced by *P. laumondii* and possess documented structures (Table 9 and Figure 14). LC-MS analyses were performed on the variants' metabolite extracts in positive mode. Subsequently, the acquired data were processed using Thermo XCalibur Qual Browser and Compound Discoverer 3.3. Expression levels of the selected compounds were then examined and normalized relative to those of *P. laumondii*-pARO190 for comparison.

DctD₍₁₄₁₋₃₉₄₎, σ^{54} -dependent pan-activating bEBP generated by Xu *et al.*³⁵ was used to assess whether σ^{54} -dependent bEBPs could regulate natural product (NP) biosynthesis in *P. laumondii*. From their *in vitro* study, Xu *et al.* concluded that the C domain of DctD interfered with transcription elongation. They reported that those transcripts were terminated shortly after activation³⁵. However, my *in vivo* results indicate an increase in metabolite expression in its presence (Figure 5). In the chromatogram of the DctD₍₁₄₁₋₃₉₄₎ variant, metabolite expression exceeds the levels of both *P. laumondii* TTO1 and *P. laumondii*-pARO190. As depicted in Figure 12, DctD₍₁₄₁₋₃₉₄₎ behaved as expected, activating the expression in a statistically significant manner in five out of the six compounds tested. The highest value was observed for PL-A, a 320%-fold change relative to the *P. laumondii*-pARO190.

Amongst the results displayed in Figure 5 and 12, we observed that the *P. laumondii*-pARO190 had an unexpected effect, activating the expression of NPs beyond the levels of the *P. laumondii* TTO1 strain. Sequencing of the empty pARO190 plasmid revealed no unexpected genetic material

(Figure 2). It was reported that during conjugation, recipient cells activate transiently their SOS response system, triggered by the increase in plasmid single-stranded DNA, resulting in an elevated mutation rate and a decrease in fitness^{47,48}. pARO190 is a high copy plasmid replicating at a rate of 500-700 copy per cell⁴⁹. Its presence at such a high concentration could have caused the activation in expression witnessed. However, further investigations are needed to determine the exact cause and its effect on growth rate. Taking this into account, we proceeded with the subsequent experiments.

The effect of mEBPs on metabolites and NPs expression were diverse and sometimes unexpected. Some variants exhibited different phenotypes despite having the same mEBP (GlrR(Δ 2-131), TyrR(Δ 2-123) and PLU_RS06090 (Δ 2-320), Table 8 and Figures 13 and 14). This discrepancy could be due to either phenotypic heterogeneity, which is well documented in *Photorhabdus*, suggesting that these isogenic bacteria modulated their gene expression in a homogeneous environment^{7,26,50}. Alternatively, this could mean that a mutation had occurred in the bacterial genome or the recombinant plasmid. Further enquiry to determine the cause of these phenotypic differences is required. Given the need for additional examination, only the general activation trend of the GlrR(Δ 2-131), and PLU_RS06090 (Δ 2-320) variants will be retained for further evaluation (Table 10).

The effects of the different mEBPs were compared to that of DctD₍₁₄₁₋₃₉₄₎, which served as standard for activated expression in *P. laumondii*. Also, as previously stated all results were standardised to the expression levels of *P. laumondii*-pARO190. Our findings reveal new and distinct results for each constitutively active mEBP: TyrR severely repressed expression, whereas PspF and GlrR generally activated expression above the levels of DctD₍₁₄₁₋₃₉₄₎. Additionally, PspF exhibited some propensity in expressing specific NPs. For PLU_RS06090 we observed what appeared to be two functions involving both activation and repression, dependent on the extent of

the deleted regulatory region. Next, we will proceed with detailed analysis of the results obtained for each of these mEBPs.

Table 10. Summary of findings for each constrictively active EBP.

mEBPs	Size	color	Metabolite expression	NPs expression	Effect on expression	Observed function
DctD ₍₁₄₁₋₃₉₄₎	normal	beige	+	+	Activation	Activator
PspF-M	normal	beige	+	+	Activation	Activator
GlrR _(Δ2-122)	normal	beige	++	+	Activation	Activator
GlrR _{(Δ2-131)Y}	normal	yellow	++	+++	Activation	
GlrR _{(Δ2-131)B}	normal	beige	++	+	Activation	
PLU_RS06090 _(Δ2-304)	normal	beige	-	+/-	Repression	
PLU_RS06090 _{(Δ2-320)Y}	normal	yellow	++	+	Activation	Two functions (activator and repressor)
PLU_RS06090 _{(Δ2-320)B}	normal	beige	++	+	Activation	
TyrR _(Δ2-200)	small	yellow	--	--	Stringent repression	Stringent repressor
TyrR _{(Δ2-123)Y}	normal	yellow	+	+	Activation	
TyrR _{(Δ2-123)B}	normal	beige	-	-	Repression	

All phenotypes are compared to DctD₍₁₄₁₋₃₉₄₎ which is considered an activator (+). All (-) score reflects values below that of *P. laumondii*-pARO190 based on observations from Table 8. For Metabolite expression, this qualitative score was based on Figure 13. For NPs expression, this quantitative score was based on Figure 14. N/A implies that the data cannot be used, further experiments are required.

The transcriptional regulatory protein TyrR is well studied in *Escherichia coli*, where it is known to regulate both repression and activation of gene expression^{51,52}. It is reported to play an important role in virulence, biofilm formation⁵², and the biosynthesis and transport of aromatic amino acids^{52,53}. In *E. coli* TyrR is recognised as being an unusual bEBP due to the absence of the GAFTGA sequence motif in its C domain, and it was shown to regulate expression through σ 70-dependent RNAP holoenzyme instead³¹. While its role in gene expression regulation in *P. laumondii* has not been extensively explored, it has been shown to play a role in the regulation of stilbene based antibiotics expression^{54,55}.

Our results have revealed a previously unreported effect of TyrR_(Δ 2-200) mEBP on transcription regulation in *P. laumondii*. This variant displayed the most impactful phenotypic

change, with the formation of small, yellow, slow growing colonies, with near-complete repression of metabolites including NPs expression (Figures 13 and 14). These findings suggest that TyrR may play an important role during the M-Form of *Photorhabdus* lifecycle, as similar phenotypes are observed during that stage²⁷.

The bEBP GlrR is reported to negatively regulate genes associated to inorganic polyphosphate synthesis in *E. coli*⁵⁶. Additionally, it plays a role in transcriptional interference by repressing expression from σ^{70} -dependent promoters in both *Salmonella* Typhimurium and *E. coli*⁵⁷. In the case of *P. laumondii*, Gopel *et al.* suggested that increased GlrR activity leads to the enhanced expression of sRNA, which regulates the expression of the GlmS enzyme responsible for producing an essential component of the bacterial cell wall⁵⁸. Our results indicated that constitutively activating GlrR has a significant activating effect on metabolite and NP expression in *P. laumondii*, which was previously undocumented (Figures 13 and 14). This demonstrates great potential in activating the expression of previously undetected NPs.

PspF, or Phage shock protein F, is a well-known transcription factor that operates as part of a response system to inner membrane (IM) stress^{59,60}. In *E. coli*, this bEBP is constitutively active (it lacks an R domain) but negatively regulated by PspA^{31,60,61}. Upon IM damage, this regulation is lifted, allowing PspF to activate the expression of *psp* genes, initiating repairs and thus preserving energy production by maintaining the balance in the proton motive force^{17,58}. However, our bioinformatic analysis indicates that in *P. laumondii* T101, PspF remains inactive due to a point mutation in the start codon. This suggests that a point mutation would be necessary for this stress response system to function, limiting its effects to the subset of the population that would naturally carry the mutation.^{7,62}

According to our findings, constitutively active PspF activates the expression of metabolites in general, although not to the extent observed with GlrR. However, it demonstrates accentuated expression in *P. laumondii* of certain analyzed NPs: anthraquinone 270, gameXpeptide A and mevalagmapeptide A (Figure 14). This suggests that PspF could be utilized to target the biosynthesis of specific NPs.

PLU_RS06090 is identified as σ^{54} -interacting transcriptional regulator found in *P. laumondii*. Little is known about the regulatory functions of this bEBP. Our results indicate that depending on the deleted region of the R domain, PLU_RS06090 exhibits different regulatory functions. When only the R elements are deleted ($\Delta 2-304$) (Table A5), it represses the expression of most metabolites and NPs (Figures 13 and 14). However, when the entire region before the C domain ($\Delta 2-320$) is removed, we observe a general activation in metabolite expression (Figure 13). These new findings suggest that PLU_RS06090 bEBP may have two functions, positively and negatively regulating genes involved in the synthesis of a wide range of metabolites including NPs. Moreover, it seems that the stretch of 16 amino acids that lies between the two deletions, codons 304 to 320, plays an important role in mediating these functions.

Our results (Table 10) highlight the efficacy of mEBPs as a tool for NP expression in *P. laumondii*. In contrast to methods like CRAGE and CRAGE-CRISPR, which successfully target specific BGCs using heterologous expression or sequential homologous recombination with specific single-guided RNA^{1,24}, our approach stands out for its ability to simultaneously target a broad range of BGCs. By harnessing the innate capacity of the native strain for secondary metabolite biosynthesis and regulation, we avoid the need for complex processes like homologous recombination, ensuring ease of implementation and scalability.

This study has uncovered many new and valuable findings that would serve as milestones in enhancing our understanding of bEBPs' regulatory function in *P. laumondii*. However, we acknowledge that certain experiments are needed to make it comprehensive. This include reducing the levels of the mEBPs expressed in the cell to ensure that the expression observed was mediated by their binding to the UAS elements present upstream of their respective genes. Also, testing the remaining 2 bEBPs, GlnG and PrpR; investigating pARO190 effect and the phenotypic variations observed within the same mEBPs; as well as performing a *rpoN* knockout experiment (for which the knockout cassettes have already been constructed) to confirm that GlrR, PspF and PLU_RS06090 alter metabolite expression via interactions with σ^{54} .

Some of these experiments are currently in progress. Marcus Simoes (MSc. candidate) is currently assessing the GlnG bEBP and conducting the *rpoN* knockout experiment using the same procedure employed in this study. Investigations regarding the PrpR($\Delta 2-208$) mEBP, pARR190 effect, and the observed phenotype discrepancies within the same mEBP (GlrR($\Delta 2-131$), TyrR($\Delta 2-123$) and PLU_RS06090 ($\Delta 2-320$)), will be assigned to future MSc. students.

The broader goal of this approach was to uncover for new NPs by activating the expression of cryptic BGCs using constitutively active bEBPs. Undergraduate students have already performed extensive screening through spot-on lawn assays to identify new bioactive compound(s), and viability assays are currently underway to assess compound toxicity. The next phase will involve conducting real-time PCR to identify if any cryptic BGCs were expressed.

In summary, our results confirm that σ^{54} -dependent bEBPs can effectively induce natural product biosynthesis, highlighting the importance of σ^{54} role as a global regulator of numerous metabolites including NPs. Additionally, GlrR and PspF, due to their activating function, hold potential for exploring new NPs with antimicrobial properties, which would aid with the ongoing struggle against antimicrobial resistance. As new findings on *P. laumondii* expression regulation, TyrR was found to acts as a stringent repressor of non-essential metabolite expression, while PLU_RS06090 was identified to potentially have two functions of repression and activation over a wide range of metabolites.

REFERENCES:

1. Wang, G. *et al.* CRAGE enables rapid activation of biosynthetic gene clusters in undomesticated bacteria. *Nat Microbiol* **4**, 2498–2510 (2019).
2. Bozhüyük, K. A. J. *et al.* Natural Products from Photorhabdus and Other Entomopathogenic Bacteria. in *The Molecular Biology of Photorhabdus Bacteria* (ed. French-Constant, R. H.) vol. 402 55–79 (Springer International Publishing, Cham, 2016).
3. Waters, C. M. & Bassler, B. L. Quorum sensing: cell-to-cell communication in bacteria. *Annu Rev Cell Dev Biol* **21**, 319–346 (2005).
4. Crawford, J. M., Portmann, C., Zhang, X., Roeffaers, M. B. J. & Clardy, J. Small molecule perimeter defense in entomopathogenic bacteria. *Proc Natl Acad Sci U S A* **109**, 10821–10826 (2012).
5. Munch, A., Stingl, L., Jung, K. & Heermann, R. Photorhabdus luminescens genes induced upon insect infection. *BMC Genomics* **9**, 229 (2008).
6. Shi, Y.-M. *et al.* Global analysis of biosynthetic gene clusters reveals conserved and unique natural products in entomopathogenic nematode-symbiotic bacteria. *Nat. Chem.* **14**, 701–712 (2022).
7. Heinrich, A. K., Glaeser, A., Tobias, N. J., Heermann, R. & Bode, H. B. Heterogeneous regulation of bacterial natural product biosynthesis via a novel transcription factor. *Heliyon* **2**, e00197 (2016).
8. Rutledge, P. J. & Challis, G. L. Discovery of microbial natural products by activation of silent biosynthetic gene clusters. *Nat Rev Microbiol* **13**, 509–523 (2015).

9. Kwon, M. J. *et al.* Beyond the Biosynthetic Gene Cluster Paradigm: Genome-Wide Coexpression Networks Connect Clustered and Unclustered Transcription Factors to Secondary Metabolic Pathways. *Microbiol Spectr* **9**, e00898-21.
10. Bode, H. B. & Müller, R. The Impact of Bacterial Genomics on Natural Product Research. *Angew. Chem. Int. Ed.* **44**, 6828–6846 (2005).
11. Tenover, F. C. Mechanisms of Antimicrobial Resistance in Bacteria. *The American Journal of Medicine* **119**, S3–S10 (2006).
12. Antimicrobial resistance : tackling a crisis for the health and wealth of nations. *Wellcome Collection* <https://wellcomecollection.org/works/rdpck35v>.
13. Blair, J. M., Richmond, G. E. & Piddock, L. J. Multidrug efflux pumps in Gram-negative bacteria and their role in antibiotic resistance. *Future Microbiology* **9**, 1165–1177 (2014).
14. La Trobe Institute for Molecular Science, Melbourne, Australia, Shafee, T., Lowe, R., & La Trobe Institute for Molecular Science, Melbourne, Australia. Eukaryotic and prokaryotic gene structure. *Wiki J Med* **4**, (2017).
15. Martinet, L. *et al.* A Single Biosynthetic Gene Cluster Is Responsible for the Production of Bagremycin Antibiotics and Ferroverdin Iron Chelators. *mBio* **10**, e01230-19 (2019).
16. Tran, P. N., Yen, M.-R., Chiang, C.-Y., Lin, H.-C. & Chen, P.-Y. Bioinformatic mining of BGC: Detecting and prioritizing biosynthetic gene clusters for bioactive compounds in bacteria and fungi. *Appl Microbiol Biotechnol* **103**, 3277–3287 (2019).
17. Scherlach, K. & Hertweck, C. Triggering cryptic natural product biosynthesis in microorganisms. *Org. Biomol. Chem.* **7**, 1753–1760 (2009).

18. Crawford, J. M., Kontnik, R. & Clardy, J. Regulating Alternative Lifestyles in Entomopathogenic Bacteria. *Current Biology* **20**, 69–74 (2010).
19. Zhu, H., Sandiford, S. K. & van Wezel, G. P. Triggers and cues that activate antibiotic production by actinomycetes. *J Ind Microbiol Biotechnol* **41**, 371–386 (2014).
20. Mao, D., Okada, B. K., Wu, Y., Xu, F. & Seyedsayamdost, M. R. Recent advances in activating silent biosynthetic gene clusters in bacteria. *Current Opinion in Microbiology* **45**, 156–163 (2018).
21. Engel, Y., Windhorst, C., Lu, X., Goodrich-Blair, H. & Bode, H. B. The Global Regulators Lrp, LeuO, and HexA Control Secondary Metabolism in Entomopathogenic Bacteria. *Front. Microbiol.* **8**, (2017).
22. Pouresmaeil, M. & Azizi-Dargahlou, S. Factors involved in heterologous expression of proteins in E. coli host. *Arch Microbiol* **205**, 212 (2023).
23. Zhang, X., Hindra & Elliot, M. A. Unlocking the trove of metabolic treasures: activating silent biosynthetic gene clusters in bacteria and fungi. *Current Opinion in Microbiology* **51**, 9–15 (2019).
24. Ke, J. *et al.* CRAGE-CRISPR facilitates rapid activation of secondary metabolite biosynthetic gene clusters in bacteria. *Cell Chemical Biology* **29**, 696-710.e4 (2022).
25. Duchaud, E. *et al.* The genome sequence of the entomopathogenic bacterium *Photorhabdus luminescens*. *Nat. Biotechnol.* **21**, 1307–1313 (2003).
26. Eckstein, S., Dominelli, N., Brachmann, A. & Heermann, R. Phenotypic Heterogeneity of the Insect Pathogen *Photorhabdus luminescens*: Insights into the Fate of Secondary Cells. *Appl Environ Microbiol* **85**, e01910-19 (2019).

27. Clarke, D. J. *Photorhabdus*: a tale of contrasting interactions. *Microbiology* **166**, 335–348 (2020).
28. Somvanshi, V. S. *et al.* A Single Promoter Inversion Switches *Photorhabdus* Between Pathogenic and Mutualistic States. *Science* **337**, 88–93 (2012).
29. Ma, M. *et al.* Identifying the Gene Regulatory Network of the Starvation-Induced Transcriptional Activator Nla28. *J Bacteriol* **204**, e00265-22.
30. Ma, M., Welch, R. D. & Garza, A. G. The σ_{54} system directly regulates bacterial natural product genes. *Sci Rep* **11**, 4771 (2021).
31. Bush, M. & Dixon, R. The Role of Bacterial Enhancer Binding Proteins as Specialized Activators of σ_{54} -Dependent Transcription. *Microbiol Mol Biol Rev* **76**, 497–529 (2012).
32. Paget, M. S. Bacterial Sigma Factors and Anti-Sigma Factors: Structure, Function and Distribution. *Biomolecules* **5**, 1245–1265 (2015).
33. Yang, Y. *et al.* Structures of the RNA polymerase-54 reveal new and conserved regulatory strategies. *Science* **349**, 882–885 (2015).
34. Buck, M., Gallegos, M.-T., Studholme, D. J., Guo, Y. & Gralla, J. D. The Bacterial Enhancer-Dependent σ_{54} (σ_N) Transcription Factor. *J Bacteriol* **182**, 4129–4136 (2000).
35. Hao Xu,^{1†} Baohua Gu,^{2‡} B. Tracy Nixon,² and Timothy R. Hoover. Purification and Characterization of the AAA+ Domain of *Sinorhizobium meliloti* DctD, a σ_{54} -Dependent Transcriptional Activator.
36. Weber, T. *et al.* antiSMASH 3.0—a comprehensive resource for the genome mining of biosynthetic gene clusters. *Nucleic Acids Res* **43**, W237–W243 (2015).

37. Rill, A., Zhao, L. & Bode, H. B. Genetic Toolbox for Photorhabdus and Xenorhabdus: pSEVA based heterologous expression systems and CRISPR/Cpf1 based genome editing for rapid natural product profiling. 2024.01.07.574529 Preprint at <https://doi.org/10.1101/2024.01.07.574529> (2024).
38. Ahmed, S., Tafim Hossain Hrithik, M., Chandra Roy, M., Bode, H. & Kim, Y. Phurealipids, produced by the entomopathogenic bacteria, Photorhabdus, mimic juvenile hormone to suppress insect immunity and immature development. *Journal of Invertebrate Pathology* **193**, 107799 (2022).
39. Heinrich, A. K., Hirschmann, M., Neubacher, N. & Bode, H. B. LuxS-dependent AI-2 production is not involved in global regulation of natural product biosynthesis in *Photorhabdus* and *Xenorhabdus*. *PeerJ* **5**, e3471 (2017).
40. Brachmann, A. O. *et al.* Pyrones as bacterial signaling molecules. *Nat Chem Biol* **9**, 573–578 (2013).
41. Muangpat, P. *et al.* Screening of the Antimicrobial Activity against Drug Resistant Bacteria of Photorhabdus and Xenorhabdus Associated with Entomopathogenic Nematodes from Mae Wong National Park, Thailand. *Front Microbiol* **8**, 1142 (2017).
42. Hapeshi, A., Benarroch, J. M., Clarke, D. J. & Waterfield, N. R. Iso-propyl stilbene: a life cycle signal? *Microbiology* **165**, 516–526 (2019).
43. Nollmann, F. I. *et al.* Insect-specific production of new GameXPeptides in photorhabdus luminescens TTO1, widespread natural products in entomopathogenic bacteria. *Chembiochem* **16**, 205–208 (2015).

44. Lewis, K. Programmed Death in Bacteria. *Microbiology and Molecular Biology Reviews* **64**, 503–514 (2000).
45. Nielsen, B. L., Willis, V. C. & Lin, C.-Y. Western blot analysis to illustrate relative control levels of the lac and ara promoters in Escherichia coli. *Biochemistry and Molecular Biology Education* **35**, 133–137 (2007).
46. Zhang, L. *et al.* Regulated gene expression in *Staphylococcus aureus* for identifying conditional lethal phenotypes and antibiotic mode of action. *Gene* **255**, 297–305 (2000).
47. San Millan, A. & MacLean, R. C. Fitness Costs of Plasmids: a Limit to Plasmid Transmission. *Microbiology Spectrum* **5**, 10.1128/microbiolspec.mtbp-0016–2017 (2017).
48. Baharoglu, Z., Bikard, D. & Mazel, D. Conjugative DNA Transfer Induces the Bacterial SOS Response and Promotes Antibiotic Resistance Development through Integron Activation. *PLOS Genetics* **6**, e1001165 (2010).
49. Parke, D. Construction of mobilizable vectors derived from plasmids RP4, pUC18 and pUC19. *Gene* **93**, 135–137 (1990).
50. Langer, A. *et al.* HexA is a versatile regulator involved in the control of phenotypic heterogeneity of *Photobacterium luminescens*. *PLoS ONE* **12**, e0176535 (2017).
51. Pittard, J. The various strategies within the TyrR regulation of Escherichia coli to modulate gene expression. *Genes Cells* **1**, 717–725 (1996).
52. Camakaris, H., Yang, J., Fujii, T. & Pittard, J. Activation by TyrR in Escherichia coli K-12 by Interaction between TyrR and the α -Subunit of RNA Polymerase. *J Bacteriol* **203**, (2021).

53. Jijón-Moreno, S., Baca, B. E., Castro-Fernández, D. C. & Ramírez-Mata, A. TyrR is involved in the transcriptional regulation of biofilm formation and D-alanine catabolism in *Azospirillum brasilense* Sp7. *PLOS ONE* **14**, e0211904 (2019).
54. Lango-Scholey, L., Brachmann, A. O., Bode, H. B. & Clarke, D. J. The Expression of *stIA* in *Photobacterium luminescens* Is Controlled by Nutrient Limitation. *PLoS ONE* **8**, e82152 (2013).
55. Bager, R., Roghanian, M., Gerdes, K. & Clarke, D. J. Alarmone (p)ppGpp regulates the transition from pathogenicity to mutualism in *Photobacterium luminescens*. *Molecular Microbiology* **100**, 735–747 (2016).
56. Bowlin, M. Q., Long, A. R., Huffines, J. T. & Gray, M. J. The role of nitrogen-responsive regulators in controlling inorganic polyphosphate synthesis in *Escherichia coli*. *Microbiology (Reading)* **168**, 001185 (2022).
57. Bono, A. C. *et al.* Novel DNA Binding and Regulatory Activities for σ^{54} (RpoN) in *Salmonella enterica* Serovar Typhimurium 14028s. *J Bacteriol* **199**, e00816-16 (2017).
58. Göpel, Y. *et al.* Common and divergent features in transcriptional control of the homologous small RNAs *GlmY* and *GlmZ* in Enterobacteriaceae. *Nucleic Acids Res* **39**, 1294–1309 (2011).
59. Mehta, P. *et al.* Dynamics and stoichiometry of a regulated enhancer-binding protein in live *Escherichia coli* cells. *Nat Commun* **4**, 1997 (2013).
60. McDonald, C., Jovanovic, G., Ces, O. & Buck, M. Membrane Stored Curvature Elastic Stress Modulates Recruitment of Maintenance Proteins *PspA* and *Vipp1*. *mBio* **6**, (2015).

61. Jovanovic, G., Lloyd, L. J., Stumpf, M. P. H., Mayhew, A. J. & Buck, M. Induction and Function of the Phage Shock Protein Extracytoplasmic Stress Response in *Escherichia coli**. *Journal of Biological Chemistry* **281**, 21147–21161 (2006).
62. Grote, J., Krysciak, D. & Streit, W. R. Phenotypic Heterogeneity, a Phenomenon That May Explain Why Quorum Sensing Does Not Always Result in Truly Homogenous Cell Behavior. *Appl. Environ. Microbiol.* **81**, 5280–5289 (2015).
63. Preparing chemically competent cells. (2023, October 24). *OpenWetWare*, . Retrieved 19:54, March 25, 2024 from https://openwetware.org/mediawiki/index.php?title=Preparing_chemically_competent_cells&oldid=1112593
64. Transforming chemically competent cells. (2012, May 17). *OpenWetWare*, . Retrieved 19:52, March 25, 2024 from https://openwetware.org/mediawiki/index.php?title=Transforming_chemically_competent_cells&oldid=603080

APPENDIX

List of supporting Figures and Tables

Figure A1. pTOX5 map from Addgene.....	50
Figure A2. Sequence alignment.	50
Figure A3. Background noise.....	53
Table A1. Primers used to confirm bEBPs' presence in <i>P. laumondii</i> TTO1.....	54
Table A2. Knockout cassette design.	54
Table A3. Primers used for the Knockout project.	55
Table A4. 22 BGCs identified in <i>P. laumondii</i> TTO1 using antiSMASH (NC_005126.1).....	56
Table A5. UniProt analysis of the Regulatory domain of <i>P. laumondii</i> bEBPs.....	57
Table A6. Observation (conjugated TTO1 colonies and LC-MS metabolite extracts).	57
Table A7. The compounds abundance (Raw data of corrected average of PH (e7))	58

Supporting Figures and Tables

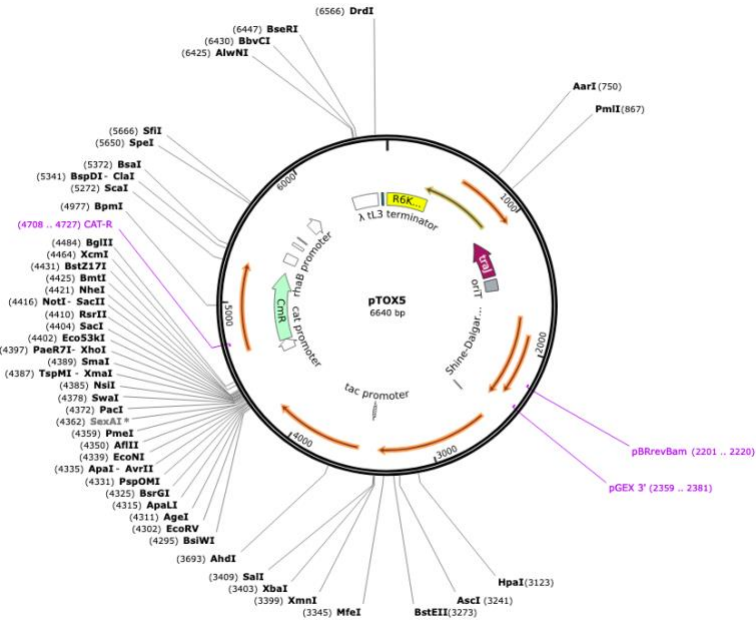


Figure A1. pTOX5 map from Addgene.

Figure A2. Sequence alignment.

Identification of the different bEBPs on *P. laumondii* TTO1 using DctD₍₁₄₁₋₃₉₄₎. (data obtained using NCBI BLASTp)

GlR bEBP.

MULTISPECIES: two-component system response regulator GlrR [Photorhabdus]						
Sequence ID: WP_011147503.1 Length: 445 Number of Matches: 1						
Range 1: 137 to 364 GenPept Graphics ▼ Next Match ▲ Previous Match						
Score	Expect	Method	Identities	Positives	Gaps	
225 bits(573) 3e-72 Compositional matrix adjust. 113/228(50%) 152/228(66%) 0/228(0%)						
Query	5	LIGQTPVMERLRQTLKHIADTDVDVLVAGETGSGKEVVATLLHQWSRRRTGNFVALNCGA	64			
		++ ++P M RL + + +A +DV VL+ G++G+GKEV+A ++ S R F+A+NCGA				
Sbjct	137	IVTRSPAMRLRLEQARMVAQSDVSVLINGQSGTGKEVLAQAIHRASPRAKKPFIAINCGA	196			
Query	65	LPETVIESELFHGHEPGAFTGAVKKRIGRIEHASGGTLFLDEIEAMPATQVKMLRVLEAR	124			
		LPE ++ESELFGH GAFTGAV R G A GGTLFLDEI MP A QVK+LRVL+ R				
Sbjct	197	LPEQLLESELFGHAKGAFTGAVSSREGLFLAAQGGTLFLDEIGDMPQALQVKLLRVLQER	256			
Query	125	EITPLGTLNLRPVDIRVVAALKVDLGDPAARGDFREDLYYRLNVTLSIPPLRERRDDIP	184			
		+I PLG+N +D+R+++A DL A+ +FREDLYYRLNVL IP L R +DIP				
Sbjct	257	KIRPLGNSNRDLIDVRIISATHRDLPKAMAKNEFREDLYYRLNVTNLKIPALNGRVEDIP	316			
Query	185	LLFSHFLARASERFGREVPASAMRAYLATHSWPGNVRELSHFAERV	232			
		LL +H L +++R V + S L SWPGNVR+L + E+				
Sbjct	317	LLANHLRESAKRHKPFVRSFSDAMKCLMAASWPGNVRQLVNVIEQC	364			

GlnN bEBP.

MULTISPECIES: nitrogen regulation protein NR(I) [Photorhabdus]
 Sequence ID: [WP_011144634.1](#) Length: 490 Number of Matches: 1

Range 1: 141 to 365 [GenPept](#) [Graphics](#) [Next Match](#) [Previous Match](#)

Score	Expect	Method	Identities	Positives	Gaps
195 bits(496)	3e-60	Compositional matrix adjust.	99/225(44%)	141/225(62%)	0/225(0%)
Query 5	LIGQTPVMERLRQTLKHIADTDVDVLVAGETGSGKEVVATLLHQWSRRRTGNFVALNCGA	64			
	+IG+ P M+ + + + ++ + + VL+ GE+G+GKE+VA LH+ S R F+ALN A				
Sbjct 141	MIGEAPAMQDVYRIIGRLSRSSISVLINGESGTGKELVAHALHRHSPRANEPFIALNMAA	200			
Query 65	LPETVIESEELFGHEPGAFTGAVKKRIGRIEHASGGTLFLDEIEAMPPATQVKMLRVLEAR	124			
	+P+ +IESEELFGHE GAFTGA + R GR E A+ G+LFLDEI MP Q ++LRVL				
Sbjct 201	IPKDLIESEELFGHEKAFTGANQVRHGRFEQANRGSFLFLDEIGDMPLDIQTRLLRVLAEG	260			
Query 125	EITPLGTNLTRPVDIRVVAAAKVDLGDPAARGDFREDLYYRLNVVTLSSIPLRERRDDIP	184			
	+ +G VD+R++AA DL +G FREDLY+RLNV+ + +PPLR+R +DIP				
Sbjct 261	QFYRVGGYAPVKVDVRIIAATHQDLERLVQKGFREDLYHRLNVIRMQLPPLRDRVEDIP	320			
Query 185	LLFSHFLARASERFGREVPASAMRAYLATHSWPGNVRELSHFA 229				
	L HFL + ++ G E + L WPGNVR+L +				
Sbjct 321	RLTRHFLQQTAKELGVETKILHPDAEIALMRLPWPGNVRQLENIC 365				

TyrR bEBP.

MULTISPECIES: transcriptional regulator TyrR [Photorhabdus]
 Sequence ID: [WP_0111446802.1](#) Length: 527 Number of Matches: 1

Range 1: 206 to 439 [GenPept](#) [Graphics](#) [Next Match](#) [Previous Match](#)

Score	Expect	Method	Identities	Positives	Gaps
186 bits(471)	2e-56	Compositional matrix adjust.	92/234(39%)	143/234(61%)	0/234(0%)
Query 5	LIGQTPVMERLRQTLKHIADTDVDVLVAGETGSGKEVVATLLHQWSRRRTGNFVALNCGA	64			
	+I +P M ++ + + +A D +L+ GETG+GK+++A H S R F+ LNC +				
Sbjct 206	IIAVSPKMAQIEQARKMAMLDAPLLIGETGTGKDILAKACHLSLRGKQPFLGLNCAS	265			
Query 65	LPETVIESEELFGHEPGAFTGAVKKRIGRIEHASGGTLFLDEIEAMPPATQVKMLRVLEAR	124			
	+P+ V+ESELFG+ GA+ A++ + G E A+GGT+ LDEI M P Q+K+LR L				
Sbjct 266	MPDDVVESELFGYAAGAYPNAIEGKGFQANGGTVLLDEIGEMSPQMQIKLLRFLNDG	325			
Query 125	EITPLGTNLTRPVDIRVVAAAKVDLGDPAARGDFREDLYYRLNVVTLSSIPLRERRDDIP	184			
	+G V++RV+ A + +L + RG+FREDLYYRLNV+ +++P LR+R+ DI				
Sbjct 326	TFRRVGEENEVKNVVRVICATQKNLVELVQRGEFREDLYYRLNVLAITLPSLRDRKTDIM	385			
Query 185	LLFSHFLARASERFGREVPASAMRAYLATHSWPGNVRELSHFAERVALGVEG 238				
	L +F+ R SE G P +S + +L ++SWPGNVR+L + R +E				
Sbjct 386	PLVEYFIERFSEEQGVKPKLSPELSHFLTSYSWPGNVRQLQNAIYRALQLEN 439				

PspF bEBP.

MULTISPECIES: phage shock protein operon transcriptional activator [Photorhabdus]
 Sequence ID: [WP_011146808.1](#) Length: 334 Number of Matches: 1

Range 1: 8 to 235 [GenPept](#) [Graphics](#) [Next Match](#) [Previous Match](#)

Score	Expect	Method	Identities	Positives	Gaps
179 bits(455)	7e-56	Compositional matrix adjust.	96/228(42%)	134/228(58%)	1/228(0%)
Query 5	LIGQTPVMERLRQTLKHIADTDVDVLVAGETGSGKEVVATLLHQWSRRRTGNFVALNCGA				64
Sbjct 8	L+G+ + + + +A V+V GE G+GKE++A LH S R G F++LNC A LLGEANSFLEILEQVSALAKLSKPVIVIGERGTGKELIARRLHYLSPRWQGPFI LNCAA				67
Query 65	LPETVIESEELFGHEPGAFTGAVKKRIGRIEHASGGTLFLDEIEAMPPATQVKMLRVLEAR				124
Sbjct 68	L E +++SEELFGHE GAFTGA K+ GR E A GGTLFLDE+ P Q K+LRV+E LNENLLDSEELFGHEAGFTGAQKRHQGRFERADGGTLFLDELATAPMQVQEKLLRVIEYG				127
Query 125	EITPLGTLNLRPVDIRVVAAAKVDLGDPAARGDFREDLYRNLNVVTL SIPPLRERRDDIP				184
Sbjct 128	+ +G + + VD R++ A +L AA+G FR DL RL ++IPPLR+R+ DI HLERVGGSQLQVDARLICATNDNLPAMAAGQFRADLLDRLAFDVVNIPLRQRQDIM				187
Query 185	LLFSHFLARASERFGREV-PAISAAMRAYLATHSWPGNVRELSHFAER				231
Sbjct 188	LL HF + + P + R L ++WPGN+REL + ER LLAQHFAIQMCRELDLPLFPGFTDQARQLQNYTWPGNIRELKNVVER				235

PrpR bEBP.

MULTISPECIES: propionate catabolism operon regulatory protein PrpR [Photorhabdus]
 Sequence ID: [WP_011147723.1](#) Length: 555 Number of Matches: 1

Range 1: 226 to 466 [GenPept](#) [Graphics](#) [Next Match](#) [Previous Match](#)

Score	Expect	Method	Identities	Positives	Gaps
176 bits(445)	2e-52	Compositional matrix adjust.	103/245(42%)	144/245(58%)	21/245(8%)
Query 7	GQTPVMERLRQTLKHIADTDVDVLVAGETGSGKEVVATLLHQWSRRRTGN-----FV				58
Sbjct 226	G + VME +R T+ A + VL+ GE+G+GKE+VA +H R G FV GDSAVMEHVRNTIMLYARSPATVLIQGESGTGKELVAQAIHHEYALRYGQVAGKHQRPFV				285
Query 59	ALNCGALPETVIESEELFGHEPGAFTGAVKK-RIGRIEHASGGTLFLDEIEAMPPATQVKM				117
Sbjct 286	A+NCGA+ E+++E+ELFG+E GAFTG+ + R G E A GTLFLDEI MP Q ++ AVNCGAIAESLLEAELFGYEEGAFTGSRGGGRAGLFEVAHRGTLFLDEIGEMPLPLQTRL				345
Query 118	LRVLEAREITPLGTLNLRPVDIRVVAAAKVDLGDPAARGDFREDLYRNLNVVTL SIPPLR				177
Sbjct 346	LRVLE + + +G + VD+R++ A DL G FR DL+YRL+V+ ++IP LR LRVLEEKSVVRVGGHRPIAVDVRIICATHCDLDTWVQDGRFRTDLFYRLSVLRINIPALR				405
Query 178	ERRDDIPLLFSHFLARA-----SERFGREVPAISAAMRAYLATHSWPGNVRELSHFA				229
Sbjct 406	ER DI +L +L RA S+ +E+ A++AY WPGNVREL + ERGHDIGILALEYLRRFAALNLPVSRVQELATCQEALQAY----HWPGNVRELRLNM				461
Query 230	ERVAL 234 ER+ L				
Sbjct 462	ERLTL 466				

PLU_RS06090 bEBP.

MULTISPECIES: sigma 54-interacting transcriptional regulator [Photorhabdus]
 Sequence ID: [WP_011145558.1](#) Length: 643 Number of Matches: 1

Range 1: 324 to 550 [GenPept](#) [Graphics](#) [Next Match](#) [Previous Match](#)

Score	Expect	Method	Identities	Positives	Gaps
194 bits(494)	8e-59	Compositional matrix adjust.	97/229(42%)	144/229(62%)	4/229(1%)
Query 5	LIGQTPVMERLRQTLKHIADTDVDVLVAGETGSGKEVVATLLHQWSRRRTGNFVALNCGA	64			
	+IG++ + ++ + +K +A TD +V++ GE+G+GKE++A +HQ S R+ + +NC A				
Sbjct 324	IIGRSASILQIEKIKVAPTANVMIIYGESGTGKELIARAIHQSSHRKQQLIRVNCAA	383			
Query 65	LPETVIESELFGHEPGAFTGAVKKRIGRIEHASGGTLFLDEIEAMPPATQVKMLRVLEAR	124			
	+P + ESE FGH GAFTGAV+ R GR E A GTLFLDEI +P Q K+LRVL+				
Sbjct 384	IPSELFEESEFFGHVKGAF TGAVRDRAGRFELADQGTFLFLDEIGEIPIELQSKLLRVLQEG	443			
Query 125	EITPLGTNLTRPVDIRVVAAAKVDLGDPAARGDFREDLYYRLNVVTL SIPLRERRDDIP	184			
	+G TR VD+R+++AA +L + FREDLY+RLNV + P LR+R++DIP				
Sbjct 444	TFERVGEEKTRHVDVRIIAATNRNLKEEVKHKRFREDLYFRLNVFPIYSPALRDRKEDIP	503			
Query 185	LLFSHFLARASERFGREVP AISAMRAY--LATHSWPGNVRELSHFAER	231			
	LL +HF ++ R++ + + R L + WPGN+REL + ER				
Sbjct 504	LLVTHFTKLICDK--RKINYL PFSQRHILELQQYDWPGNIRELQNVIER	550			

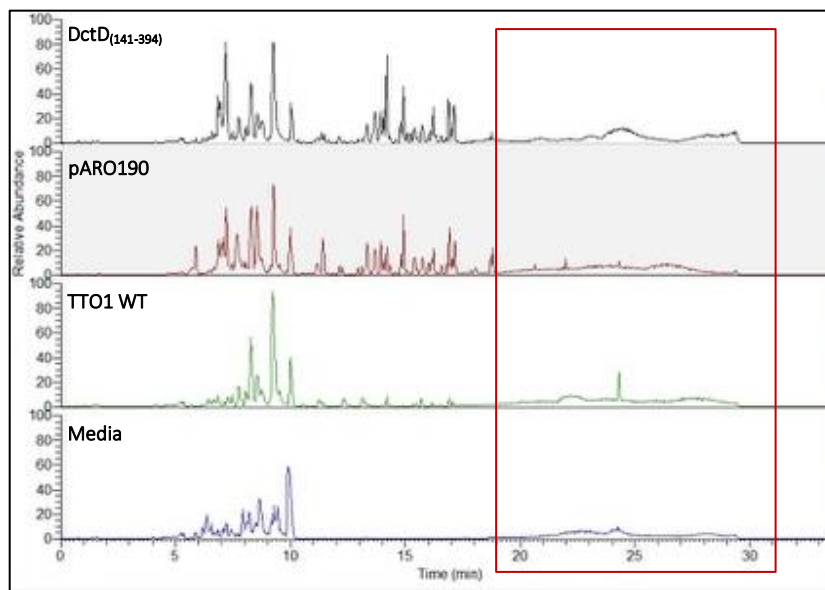


Figure A3. Background noise.

Chromatograms of different samples indicating the presence of background noise. The y axis indicates the relative abundance (PH) at a scale of **7.00 E8**. The x axis indicates the elution time in minutes of the different metabolites. The red box indicates the area from 19 min on, that displays strong background noise and indistinguishable peaks. Data from Xcalibure analysis software.

		ATTTGCAGGTGATGTCATGCCAAAAGACAAATAAAAAACGGTCTCTATCTGAATTTA ATGAACGGATAACTCATAAAAAATTAATTAATTAACGC
Plu2733- KC	1 st RE EcoRV; 1 st HA; J23100 promoter in red; Km ^r ; 2 nd HA; 2 nd RE Pacl	<u>GATATCCGTGGAGCCGCACAATAATGGAATATAATAACA</u> ACTATTGGCCGTTGAAT TATACACAGCTCCGCTTAGCTATTGCTAATACTGTTGCTGACGATAAGTCtaga GTTG ACGGCTAGCTCAGTCTTAGGTACAGTGTAGCT tctaga GAAAGAGGGGACA Aactagat gagccatattcaacgggaaacgctctgcttagcggcggataaattccaacatggatgctgatttatgggtataaatgggctcgcgataa tgcgggcaatcaggtgcaaatctatcattgatgggaagcccgatgcccagagttgtttcgaacatgccaagagtagcgttccc aatgatgtacagatgagatggtcagactaaactggctgacggaatttatgctctccaccatcaagcattttaccgtactcctgatgatg catggtactcaccactcggatccccgggaaaacagcattccaggtattagaagaatctctgattcaggtgagaatattgtgatcgctg gcagttctctgcccgttgcattcattctgttttaattgctctttaacagcagcgcgatttctctcctcagcggcgaatcacgaat gaataacgggttgggtgatcgagtgattttgatgacgagcgtaatggctggcctgttgaacaagctcggaaagaaatcataaactttgcc attctcaccggattcagtcgactcatggtgatttctactgataacctattttgacgaggggaaataataggttattgatgttgacga gtcggatcgcagacgataaccaggatcttccatcctatggaactgcctcggtagttttctcctcattacagaacggcttttcaaaaat atggtattgataatctgatatgaataaattcagtttcattgatgctcaggtttttctaaagTGGGGCTGTTTTTGATTGA TTTATTGGATTGCATAGGCACTCAGCATAACTTGATGCCTGGTGATACGGAACGAT AACAAATCGTAAAAATGGATGCTGATTTAATTAACGC
Plu3534- KC	1 st RE EcoRV; 1 st HA; J23100 promoter in red; Km ^r ; 2 nd HA; 2 nd RE Pacl	<u>CGATATCAATCACCACCTCGGTTACCTCATATTCTGCCACTACAGCCCCAATTGACTT</u> GTTACGTTGAATAAACCATTCTTTTTCAAGCCAATCACATAACTGTTCTAtaga GTTGA CGGCTAGCTCAGTCTTAGGTACAGTGTAGCT tctaga GAAAGAGGGGACA Aactagtgag ccatattcaacgggaaacgctctgcttagcggcggataaattccaacatggatgctgatttatgggtataaatgggctcgcgataatgc gggcaatcaggtgcaaatctatcattgatgggaagcccgatgcccagagttgtttcgaacatgccaagagtagcgttccaatg atgttacagatgagatggtcagactaaactggctgacggaatttatgctctcctcagaccataagcattttaccgtactcctgatgatgctg gttactcaccactcggatccccgggaaaacagcattccaggtattagaagaatctctgattcaggtgagaatattgtgatcgctggcag tgtcctgcccgggttcattcattcctgtttgaattgctctttaacagcagcgtatttctcctcagcggcgaatcacgaatgaata acgggttgggtgatgctgagtgattttgatgacgagcgtaatggctggcctgttgaacaagctcggaaagaaatcataaactttgccattctc accgattcagtcgactcatggtgatttctactgataacctattttgacgaggggaaataataggttattgatgttgagcagatcg gaatcgcagaccgataaccaggtcttgcctcctatggaactgcctcggtagttttctcctcattacagaacggcttttcaaaaatag tattgataatcctgatatgaataaattgcagtttcattgatgctcaggtttttctaaagGGGAAGTGAGTGCCCTTAAGT TTGAACCTTAACCTACCATCTTTACTAAACAGCAATACTCCCTGCTCGTAAGCATCT TGGACTAATTCAGCATATCCAATTAATTAACGC
KC : knockout cassette; FW : forward primer; RC : reverse complement primer; RE: restriction enzyme; 1 st HA : homologous arm at the gene start; 2 nd HA : homologous arm at the gene end; Km ^r : kanamycin resistance.		

Table A3. Primers used for the Knockout project.

Name	Function	Modifications & Sequences
FW: rpoN-KC	Amplify the KC	GATATCGCCAGGAGAATTGATTTAACGC
RC: rpoN-KC	Amplify the KC	TTAATTAATTTGTCTTCTTCTCTGTTC
FW: Plu1113-KC	Amplify the KC	GATATCAATTAATGATATTATCCTCAGC
RC: Plu1113-KC	Amplify the KC	TTAATTAATAAAGATTACCTCAAGTCGTG
FW: Plu1213-KC	Amplify the KC	GATATCGTGGATAAAAAAATGACAACATG
RC: Plu1213-KC	Amplify the KC	TTAATTAATTAATTTTTATGAGTTATCCGTTT
FW: Plu2733-KC	Amplify the KC	GATATCCGTGGAGCCGCACAATAATG
RC: Plu2733-KC	Amplify the KC	TTAATTAATCAGCATCCATTTTACGATTTG
FW: Plu3534-KC	Amplify the KC	GATATCAATCACCACCTCGGTTACCTCATATTC
RC: Plu3534-KC	Amplify the KC	TTAATTAATGGATATGCTGAAATTAAGTCCAAG
FW: rpoN	Confirm knockout	TCAGGCTTAGTCAGCAACTGG
RC: rpoN	Confirm knockout	TGTTTCATTTCAAACCGAGACGCC
FW: Plu1113	Confirm knockout	ATCCTCAGCTCAATGAAATAGAAAAG
RC: Plu1113	Confirm knockout	AGGGAAAAGTTCAATAACGCGG
FW: Plu1213	Confirm knockout	CGTGAATACTGGCTGATGCG
RC: Plu1213	Confirm knockout	TGCTCTTTTGGCATGACATCAC
FW: Plu2733	Confirm knockout	TGGAGCCGCACAATAATGGA
RC: Plu2733	Confirm knockout	CCGATCACCAGGCATCAAGT
FW: Plu3534	Confirm knockout	ATATTCTGCCACTACAGCCCC
RC: Plu3534	Confirm knockout	AAGATGCTTACGAGCAGGGAG
KC : knockout cassette; FW : forward primer; RC : reverse complement primer.		

Table A4. 22 BGCs identified in *P. laumondii* TTO1 using antiSMASH (NC_005126.1)

Region	Most similar known cluster	Similarity
1		
2	1-carbapen-2-em-3-carboxylic acid	41%
3		
4		
5	mevalgmapeptide A/ mevalgmapeptide B/ mevalgmapeptide C/ mevalgmapeptide D	95%
6	endopyrrole B/ endopyrrole A	50%
7	malonomycin	11%
8		
9	O-antigen	14%
10	luminmycin A/ glidobactin A/ cepafungin	100%
11	minimycin	80%
12	HTTPCA/ prepiscibactin/ piscibactin	97%
13	kolossin	100%
14	frederiksenibactin	23%
15	gameXpeptide A/ gameXpeptide B/ gameXpeptide E/ luminmide B/ luminmide D/ luminmide E/ luminmide F/ luminmide G	13%
16	gameXpeptide A/ gameXpeptide B/ gameXpeptide E/ luminmide B/ luminmide D/ luminmide E/ luminmide F/ luminmide G	94%
17		
18	odilorhabdin NOSO-95A/ odilorhabdin NOSO-95B/ odilorhabdin NOSO-95C	70%
19		
20	anthelvencin A/ anthelvencin B/ anthelvencin C	13%
21	carotenoid	83%
22	putrebactin/ avaroferrin	100%
23	conglobatin	10%

Table A5. UniProt analysis of the Regulatory domain of *P. laumondii* bEBPs.

bEBPs	Regulatory elements	Codon position
PspF	N/A	N/A
PLU_RS06090	PAS and PAC	169 to 237 and 241 to 292
GlrR	Response regulatory (RR)	8 to 122
TyrR	ACT and PAS	2 to 72 and 78 to 123
PrpR	unidentified regulatory domain	-

Table A6. Observation (conjugated TTO1 colonies and LC-MS metabolite extracts).

Samples' name	Colony color	Colony round shape/growth	Volume extracted	Beads color	Extract color	Pellet color
Media (control #4, p182)	N/A	N/A	700ul	-	-	Light yellow
TTO1 WT (Plum TTO1 phase I, p186)	Beige	Round, regular	700ul	Light beige	-	Brown/deep orange
pAro190 (pAro190#1, p135)	Beige	Round, regular	-	-	-	-
pAro190 (pAro190#2, p135)	Beige	Round, regular	-	-	-	-
pAro190 (pAro190#3, p135)	Beige	Round, regular	-	-	-	-
dctD (tDctD/LR 1#1, p179)	Beige	Round, regular	950ul	-	Deep orange	Brown/deep orange
dctD (tDctD/LR 1#2, p179)	Beige	Round, regular	800ul	-	Deep orange	Brown/deep orange
dctD (tDctD/LR 1#3, p179)	Beige	Round, regular	950ul	-	Deep orange	Brown/deep orange
pspF (pspF-M#1, p98)	Beige	Round, regular	850ul	Brown/deep orange	-	-
pspF (pspF-M#2, p98)	Beige	Round, regular	850ul	Brown/deep orange	-	-
pspF (pspF-M#3, p98)	Beige	Round, regular	850ul	Brown/deep orange	-	-
PAS 304 (uPAS-D2-304#1, p98)	Beige	Round, regular	850ul	Light orange	-	-
PAS 304 (uPAS-D2-304#2, p98)	Beige	Round, regular	850ul	Light orange	-	-
PAS 304 (uPAS-D2-304#3, p98)	Beige	Round, regular	850ul	Light orange	-	-
PAS 320-Y (uPAS-D2-320 3-1, p186)	Yellow	Round, regular	700ul	-	Light orange	Brown/deep orange
PAS 320-Y (uPAS-D2-320 3-2, p186)	Yellow	Round, regular	700ul	-	Light orange	Brown/deep orange
PAS 320-Y (uPAS-D2-320 3-3, p186)	Yellow	Round, regular	700ul	-	Light orange	Brown/deep orange
PAS 320-B (uPAS-D2-320 1-1, p186)	Beige	Round, regular	700ul	Orange	Orange	Brown/deep orange
PAS 320-B (uPAS-D2-320 1-2, p186)	Beige	Round, regular	630ul	Orange	Orange	Brown/deep orange
PAS 320-B (uPAS-D2-320 1-3, p186)	Beige	Round, regular	700ul	Orange	Orange	Brown/deep orange
glrR 122 (glrR-D2-122 1#1, p179)	Beige	Round, regular	950ul	-	Light orange	Brown/deep orange

glrR 122 (glrR-D2-122 1#2, p179)	Beige	Round, regular	950ul	-	Light orange	Brown/deep orange
glrR 122 (glrR-D2-122 1#3, p179)	Beige	Round, regular	800ul	-	Light orange	Brown/deep orange
glrR 131-Y (glrR-D2-131 1-1, p186)	Yellow	Round, regular	700ul	-	Deep orange	Brown/deep orange
glrR 131-Y (glrR-D2-131 1-2, p186)	Yellow	Round, regular	700ul	-	Deep orange	Brown/deep orange
glrR 131-Y (glrR-D2-131 1-3, p186)	Yellow	Round, regular	700ul	-	Deep orange	Brown/deep orange
glrR 131-B (glrR-D2-131 5-1, p186)	Beige	Round, regular	700ul	Orange	Light orange	Brown/deep orange
glrR 131-B (glrR-D2-131 5-2, p186)	Beige	Round, regular	700ul	Orange	Light orange	Brown/deep orange
glrR 131-B (glrR-D2-131 5-3, p186)	Beige	Round, regular	700ul	Orange	Light orange	Brown/deep orange
tyrR 123-Y (tyrR-D2-123 5-1, p182)	Yellow	Round, regular	700ul	-	-	Deep orange
tyrR 123-Y (tyrR-D2-123 5-2, p182)	Yellow	Round, regular	700ul	-	-	Deep orange
tyrR 123-Y (tyrR-D2-123 5-3, p182)	Yellow	Round, regular	700ul	-	-	Deep orange
tyrR 123-B (tyrR-D2-123 6-1, p182)	Beige	Round, regular	700ul	-	-	clear yellow
tyrR 123-B (tyrR-D2-123 6-2, p182)	Beige	Round, regular	700ul	-	-	clear yellow
tyrR 123-B (tyrR-D2-123 6-3, p182)	Beige	Round, regular	700ul	-	-	clear yellow
tyrR 200 (tyrR-D2-200#1, p98)	Yellow	Very small/slow	850ul	Yellow	-	-
tyrR 200 (tyrR-D2-200#2, p98)	Yellow	Very small/slow	850ul	Yellow	-	-
tyrR 200 (tyrR-D2-200#3, p98)	Yellow	Very small/slow	850ul	Yellow	-	-

Table A7. The compounds abundance (Raw data of corrected average of PH (e7))

Variants	PL-A	AQ 270	PPY-D	GXP-A	IPS	MVAP-A
DctD _(Δ141-394)	6.18	1.24	8.67	11.24	20.03	60.89
P.lau-pARO190	1.93	0.58	5.32	9.50	18.87	38.93
P.lau WT	0.88	0.24	4.21	6.61	1.91	7.19
pspF-M	3.89	1.49	6.78	14.12	17.10	81.40
PLU_RS06090 _(Δ2-304)	0.18	0.26	0.72	7.86	1.13	1.26
PLU_RS06090 _(Δ2-320) B	6.05	1.19	4.13	19.82	34.80	64.17
PLU_RS06090 _(Δ2-320) Y	3.86	0.66	11.55	18.05	27.14	88.44
glrR _(Δ2-122)	5.05	0.96	9.72	14.24	20.45	69.06
glrR _(Δ2-131) Y	6.85	1.33	12.41	17.42	25.65	89.48
glrR _(Δ2-131) B	4.87	0.81	10.01	16.15	31.30	69.85
tyrR _(Δ2-123) Y	3.80	0.88	13.13	13.25	21.13	79.53
tyrR _(Δ2-123) B	0.14	0.00	2.09	11.68	1.17	0.34
tyrR _(Δ2-200)	0.00	0.00	0.00	4.82E-03	0.00	0.00